Current Research in Microbial Sciences 3 (2022) 100148

Contents lists available at ScienceDirect

Current Research in Microbial Sciences

journal homepage: www.sciencedirect.com/journal/current-research-in-microbial-sciences

The H_2O_2 inherently released by the mycobacterial minor subpopulation enhances the survival of the major kin subpopulation against rifampicin

Rashmi Ravindran Nair [a,b], Deepti Sharan [a,c], Vijay Srinivasan [a,d], Nagaraja Mukkayyan [a,e], Kishor Jakkala [a,f], Parthasarathi Ajitkumar [a,*]

[a] Department of Microbiology and Cell Biology, Indian Institute of Science, Bangalore 560012, Karnataka, India
[b] Department of Microbiology, University of Alabama at Birmingham, Birmingham, Alabama, USA
[c] Department of Microbiology, University of Chicago, Chicago, IL 60637, USA
[d] School of Physics and Astronomy, University of Edinburgh, Edinburgh, UK
[e] Department of Microbial Pathogenesis, University of Maryland, Baltimore 21201, Maryland, USA
[f] Department of Microbiology and Immunology, Emory University School of Medicine, Atlanta, Georgia, USA

ARTICLE INFO

Keywords:
Mycobacteria
Bacterial subpopulations
Rifampicin
Isoniazid
H_2O_2
Antibiotic stress
Oxidative stress
Survival

ABSTRACT

Exposure to antibiotics most often generates oxidative stress in bacteria. Oxidative stress survival mechanisms would facilitate the evolution of antibiotic resistance. As part of an effort to understand oxidative stress survival mechanisms in mycobacteria, here we show that the minor subpopulation (**SC**s; **s**hort-sized **c**ells constituting 10% of the population) of *Mycobacterium smegmatis* significantly increased the survival of its major kin subpopulation (**NC**s; **n**ormal/long-sized **c**ells constituting 90% of the population) in the mid-log-phase (MLP) cultures against the oxidative stress induced by rifampicin and exogenously added H_2O_2 (positive control). We had earlier shown that the SCs in the MLP cultures inherently and naturally release significantly high levels of H_2O_2 into the medium. Addition of the SCs' culture supernatant, unlike the supernatant of the dimethylthiourea (H_2O_2 scavenger) exposed SCs, enhanced the survival of NCs. It indicated that NCs' survival required the H_2O_2 present in the SCs' supernatant. This H_2O_2 transcriptionally induced high levels of catalase-peroxidase (KatG) in the NCs. The naturally high KatG levels in the NCs significantly neutralised the endogenous H_2O_2 formed upon exposure to rifampicin or H_2O_2, thereby enhancing the survival of NCs against oxidative stress. The absence of such enhanced survival in the *furA-katG* and *katG* knockout (KO) mutants of NCs in the presence of wild-type SCs, confirmed the requirement of the H_2O_2 present in the SCs' supernatant and NCs' KatG for enhanced oxidative stress survival. The presence of SCs:NCs at 1:9 in the pulmonary tuberculosis patients' sputum alludes to the clinical significance of the finding.

1. Introduction

Bacterial subpopulations survive high concentrations of antibiotics despite majority succumbing to the sterilising activity. The small antibiotic-surviving population could acquire SOS driven genetic mutations, grow and divide in the continued presence of the antibiotic, establishing a mutant population (Woodford and Ellington, 2007). However, there are other diverse mechanisms by which bacterial populations survive in the presence of antibiotics, often even without acquiring mutation (Hui et al., 1977; Bentrup and Russell, 2001; Sarathy et al., 2012; Blair et al., 2015; Brauner et al., 2016; Ehrt et al 2018; Nicoloff et al., 2019; Sebastian et al., 2020). Several studies have shown antibiotic surviving population to be a potential reservoir of viable cells from which antibiotic resisters emerge *de novo* (Cohen et al., 2013; Sebastian et al., 2017; Swaminath et al., 2020). Reports from several groups had demonstrated generation of oxidative stress in the antibiotic surviving populations of *Escherichia coli* and *Staphylococcus aureus* (Kohanski et al., 2010; Dwyer et al., 2014; Hoeksema et al., 2018; Paul et al., 2021), mycobacteria (Piccaro et al., 2014; Sebastian et al., 2017; Swaminath et al., 2020; Paul et al., 2022), and other bacteria of

Abbreviations: CFU,, colony forming unit; LB,, Luria-Bertani; HRP,, horse radish peroxidase; PCR,, polymerase chain reaction; GFP,, green fluorescence protein; AES,, allelic exchange substrates; SCs,, short-sized cells; NCs,, normal/long-sized cells; SCF,, SCs-enriched fraction; NCF,, NCs-enriched fraction; MLP,, Mid-log-phase; NLP,, Natural-like Proportion; DMTU,, dimethylthiourea; ROS,, reactive oxygen species.

* Corresponding author.
E-mail address: ajitkpartha@gmail.com (P. Ajitkumar).

https://doi.org/10.1016/j.crmicr.2022.100148
Received 6 December 2021; Received in revised form 4 June 2022; Accepted 15 June 2022
Available online 18 June 2022

diverse genera (Albesa et al., 2004). However, antibiotics exposure need not invariably generate oxidative stress as reported in the exposure of mycobacteria against kanamycin, norfloxacin, or streptomycin (McBee et al., 2017). Although oxidative stress is often generated during antibiotic exposure, whether this results in bacterial cell death remains debatable (Keren et al., 2013; Liu and Imlay, 2013). Nevertheless, all these studies reported generation of oxidative stress in the antibiotic exposed condition but not in the natural unstressed actively growing condition.

In this regard, we reported the presence of a minor subpopulation of **s**hort-sized **c**ells (SCs; ~10% of the whole population), in the mid-log phase (MLP) cultures of *Mycobacterium tuberculosis* (*Mtb*), *Mycobacterium smegmatis* (*Msm*), *Mycobacterium xenopi* (*Mxe*) and in the tubercle bacilli in the sputum of pulmonary tuberculosis patients, with significantly and naturally high oxidative stress (Vijay et al., 2014a, b; Vijay et al., 2017). The major subpopulation of **n**ormal/long-sized **c**ells (NCs; ~90% of the whole population) showed low oxidative stress. The high oxidative stress rendered *Mtb/Msm* SCs significantly susceptible to rifampicin, isoniazid, and oxidative/nitrite stress (Vijay et al., 2017; Nair et al., 2019a). The high oxidative stress was due to significantly elevated natural levels of superoxide in SCs, due to high levels of NADH oxidase activity (Nair et al., 2019a, b). Consequentially, SCs contained significantly high levels of H_2O_2, due to superoxide dismutase activity, high levels of Fe (II) due to damage of 4Fe-4S proteins caused by the ROS, and elevated levels of hydroxyl radical due to Fenton reaction between H_2O_2 and Fe (II). The high ROS levels significantly increased SCs' antibiotic resister generation frequency, despite causing enhanced susceptibility to rifampicin/isoniazid/H_2O_2. The SCs released significantly high levels of H_2O_2 into the medium (Nair et al., 2019b). The inherently high H_2O_2 levels in the SCs' culture supernatant elevated antibiotic resister generation frequency of NCs in the MLP cultures where the SCs and NCs co-existed at 1:9 ratio (Nair et al., 2019b). The antibiotic resister frequency enhancement is a novel role of H_2O_2, like its sensing, signaling, or transcription regulatory role during physiological stress in bacteria and eukaryotes (Groeger et al., 2009; Marinho et al., 2014; Sies, 2017; Erttmann and Gekera, 2019).

In view of these observations, we wanted to find out whether the high levels of H_2O_2 released naturally and inherently into the medium by SCs would enhance NCs' survival and hence of the whole combined NCs-SCs (90%:10%) population against rifampicin, isoniazid, and H_2O_2 (positive control). Here we report the phenomenon and its mechanism by which the significantly high levels of H_2O_2 in the culture supernatant of the unstressed SCs enhanced the survival of NCs and therefore of NCs-SCs (90%:10%) whole population against rifampicin and H_2O_2, but not isoniazid. The high levels of H_2O_2 released by SCs and the H_2O_2-recipient NCs showed enhanced susceptibility to isoniazid which is an oxidative activation requiring prodrug. This hinted the involvement of oxidative processes in the mechanism of enhanced survival of NCs promoted by SCs against rifampicin/H_2O_2.

2. Materials and methods

For ease of understanding, the following terms are defined:

SCs: short-sized cells; NCs: normal/long-sized cells; SCF: SCs-enriched fraction; NCF: NCs-enriched fraction; MLP: Mid-log-phase; NLP: Natural-like Proportion.

2.1. Bacterial strains and culture conditions

M. smegmatis mc^2155 (*Msm*) (Snapper et al., 1990) cultures (Table S1) were grown in Middlebrook 7H9 broth containing 0.05% v/v Tween 80, at 37°C, with shaking at 170 rpm, till the $OD_{600\ nm}$ of the culture reached 0.6 (mid-log phase, MLP). For determining the CFU, the mycobacterial cells were plated on Middlebrook 7H10 or Mycobacteria 7H11 agar and incubated at 37°C for 3 days for the colonies. *Escherichia coli* JM109 and JC10289 strains (Table S1) were cultured in Luria-Bertani (LB) broth or LB agar (Difco). *E. coli* JC10289 containing pJV53 and pYUB854 were grown on Luria Bertani agar containing kanamycin (25 μg ml^{-1}) and hygromycin (150 μg ml^{-1}), respectively.

2.2. Size-based fractionation of mycobacterial cells using preparative scale Percoll gradient centrifugation

The Percoll density gradient was set up manually from 64% to 80% to obtain enriched fractions of short-sized cells (SCs-enriched fraction, SCF) and normal/long-sized cells (normal/long-sized cell enriched fraction, NCF), as described (Nair et al., 2019b). The detailed procedure of the preparation and processing of Msm SCF1, SCF2, and NCF cells are given under "Supplementary Materials and Methods".

2.3. Preparation of the different proportionate mixtures of SCF and NCF

The different proportionate mixtures were made in the same manner, as described (Nair et al., 2019b). A v/v/v ratio of 1:1:5 mixture of SCF1: SCF2:NCF cells was found to give rise to a proportion similar to that exists in MLP, which was called NLP. For the preparation of Un-Natural Proportion 1, the SCF1, SCF2, and NCF were mixed back at the 1:1:1 v/v/v proportion. Likewise, the Un-Natural Proportion 2 (1:1:2 v/v/v) and Un-Natural Proportion 3 (2:2:1 v/v/v) mixtures were also prepared (Fig. S1A and B). Equal volumes (100 μl each) of the cells from all the nine (64, 66, 68, 70, 72, 74, 76, 78, and 80%) Percoll fractions were mixed to obtain the Total Reconstituted Population. Each of the samples was plated to determine the CFU ($n = 10$). The details of the preparation of the different proportionate mixtures are given under "Supplementary Materials and Methods".

2.4. Determination of the percentage survival of cells against stress

The percentage survival of the cells in the different samples against antibiotics and oxidative stress was determined by plating the cells before the exposure to stress (i.e., at 0 hr) and after the exposure to stress (1 hr, 4 hrs and 6 hrs for H_2O_2, rifampicin and isoniazid exposure, respectively) followed by incubating the plates at 37°C in bacteriological incubator. The experiments were repeated using 10 biological replicates. Statistical significance was calculated using paired two-tailed *t*-test.

2.5. Exposure of NCF cells to the supernatant from the unexposed and DMTU-exposed SCF cells

The unexposed/ DMTU-exposed SCF cells, equivalent to its proportion present in NLP, were added into 25 ml Middlebrook 7H9 broth in 100 ml flask and the supernatant was collected. The NCF cells, equivalent to its proportion present in NLP, were then added to the previously collected SCF supernatant. To compare the effect of SCF supernatant on NCF cells, equivalent number of NCF cells were also added into 25 ml Middlebrook 7H9. Subsequently, the samples were exposed to 25 μg ml^{-1} rifampicin and incubated under shaking conditions at 170 rpm, 37°C for 4 hrs. The CFU of the samples was determined by plating before (i. e., at 0 hr) and after the stress duration followed by incubation of the plates at 37°C for 3-4 days. The details of the procedures are described under "Supplementary Materials and Methods".

2.6. Total RNA preparation from Msm cells

Total RNA from the NCF and NLP cells were isolated using hot phenol method, as described (Wecker, 1959; Ausubel and Kingston, 1987) with slight modifications for mycobacterial cultures, as described under "Supplementary Materials and Methods". The final RNA pellet was air-dried at 25°C, dissolved in 20 μl of DEPC-treated water, quantitated using NanoDropTM 1000 Spectrophotometer (Thermo Fisher Scientific), and stored at −70°C.

2.7. cDNA preparation for real-time PCR

Preparation of cDNA from each gene was carried out using 100 ng of total RNA from the different populations, as described (Nair et al., 2019b). The detailed protocol for the cDNA preparation is given under "Supplementary Materials and Methods".

2.8. Real time PCR

RT-qPCR experiments were performed using Real Time PCR Eva-Green Mastermix (G-Biosciences). The analysis was performed using the comparative ΔΔCt method (Wang et al., 2006), followed by normalisation (Willems et al., 2008). The primers for RT-qPCR are given in Table S2A. The detailed procedure for RT-qPCR is given under "Supplementary Materials and Methods".

2.9. Western blotting for KatG protein

Protein was initially isolated from the unexposed NCF/NLP cells. The KatG levels in the NCF/NLP cells were detected using mouse monoclonal antibody generated against mycobacterial KatG (Cat. No. NR-13793; BEI Resources) and HRP-conjugated IgG secondary antibody (product no: A 5906, Sigma, raised in sheep). The quantification of the Western blots was performed by densitometry (Fujifilm LAS-1000). Statistical significance was calculated using paired two-tailed *t*-test. The detailed procedure of western blotting is given under "Supplementary Materials and Methods".

2.10. Cloning of furA-katG promoter and genome integration

The *furA* gene (*MSMSEG_6383*) sequence was analysed and the segment predicted to have promoter activity was amplified using High fidelity Phusion DNA polymerase (Thermo Fisher Scientific) from the *Msm* genome with Msm-furAkatGprom-XbaI and Msm-furAkatGprom-KpnI specific primers with XbaI and KpnI restriction sites, respectively (Table S2B). The amplified sequence was double digested, gel purified and cloned in pBS-KS using XbaI and KpnI sites for sequence verification. The promoter segment was then subcloned in pAKMN2-*ugfp*$_m^{2+}$ vector as 5′ transcriptional fusion to the reporter gene *ugfp*$_m^{2+}$ (Roy et al., 2012; Sebastian, 2016). *Msm* cells were electroporated with the recombinant pAKMN2-P$_{MSMEG_6383}$-*ugfp*$_m^{2+}$ vector. The clones were confirmed by PCR amplification with Taq DNA polymerase (Thermo Fisher Scientific) using mycgfp2-RT-f and mycgfp2-RT-r primers (Table S2A). The detailed procedure of *furA-katG* promoter cloning is given under "Supplementary Materials and Methods".

2.11. Flow cytometry of Msm/PfurA-katG-ugfp$_m^{2+}$ samples

The *Msm/PfurA-katG-ugfp*$_m^{2+}$ and *Msm* WT cells were grown in Middlebrook 7H9 media till the cultures reached MLP. Following Percoll density gradient centrifugation of the *Msm/PfurA-katG-ugfp*$_m^{2+}$ and *Msm* WT cells, two NLP samples were prepared in the following cross mixtures: SCF WT with NCF/*PfurA-katG-ugfp*$_m^{2+}$ and DMTU-exposed SCF WT with unexposed NCF/*PfurA-katG-ugfp*$_m^{2+}$. These samples were then subjected to flow cytometry analysis. Data was acquired using Becton Dickinson FACSVerse flow cytometer with a 488 nm solid state laser and a 527/32 nm emission filter (GFP) at medium flow rate. The median fluorescence of the samples was normalised with their respective autofluorescence controls. Statistical significance was calculated using Students' *t*-test. A detailed protocol of the flow cytometry of *Msm/PfurA-katG-ugfp*$_m^{2+}$ samples is given under "Supplementary Materials and Methods".

2.12. Generation of furA-katG and katG knockout mutants of Msm cells and exposure to stress

For the construction of the recombinant plasmids containing allelic exchange substrates (AESs), cloning was carried out, as described, (van Kessel and Hatfull, 2007) and the AESs were prepared using the protocol (Bibb and Hatfull, 2002) with slight modifications. The restriction endonuclease (RE) sites for the directional cloning of the homologues flanking regions (here onwards 'homologues flanking regions' called as 'flank') in pYUB854 plasmid were incorporated at the 5' end of all the primers used in the AESs. The list of the primers used is in Table S2C. *E. coli* JC10289 for the transformation and the plasmids for the construction of AESs were prepared, as described (Sambrook and Russell, 2001). The detailed protocol of the generation of the *furA-katG and katG* knockout strains is given under "Supplementary Materials and Methods".

2.13. Exposure of Msm wild type (WT) and furA-katG and katG knockout mutants to rifampicin/H_2O_2

The NCF and NLP cells of *Msm* WT and KO were exposed to 25 μg ml^{-1} rifampicin for 4 hrs or 0.8 mM H_2O_2 for 1 hr in 25 ml Middlebrook 7H9 broth taken in 100 ml flask and kept under shaking condition at 170 rpm and 37°C. The percentage survival was determined by plating the cells before and after the exposure to the stress conditions, as described earlier. Statistical significance was calculated using paired two-tailed *t*-test.

2.14. Statistical analysis of the survival of the different proportionate mixtures during exposure to rifampicin/H_2O_2

The statistical significance of the pairwise differences in the percentage survival of the different proportionate mixtures, the NLP and NCF cells of WT and KO was analysed using the parametric paired *t*-test. Since the different proportionate mixtures needed to be compared with the NCF obtained from the same culture, the paired *t*-test (using GraphPad Prism) was employed (Vijay et al., 2017).

3. Results

3.1. Experimental rationale and strategy

To test whether SCs could enhance survival of NCs through H_2O_2, we first isolated them as enriched subpopulations using Percoll density gradient centrifugation, as described by us (Vijay et al., 2017). These were the **SC**s-enriched **f**raction (**SCF**) and the **NC**s-enriched **f**raction (**NCF**), which were viable as they grew and divided in ~3 hr (generation time) in fresh Middlebrook 7H9 medium to give an MLP-like population, as reported by us (Vijay et al., 2014a, b; Vijay et al., 2017). Since the SCs (10% of MLP) got enriched into two Percoll fractions, the SCF1 (~78% enriched in the fraction) and SCF2 (~75% enriched in the fraction), they were combinedly used as SCF, as described (Vijay et al., 2017). The NCF showed ~68% enrichment of NCs in the fraction (Vijay et al., 2017). At times, the individual role of SCF1 and SCF2 was also assayed. Percoll fractionation did not affect the viability or stress response of SCF/NCF, as earlier found by us (Vijay et al., 2017). It may be noted that the mycobacterial cells elongate to twice their length before the cell division. Under normal conditions of growth, the SCs grow and divide to give again a normal mid-log phase population consisting of 90% NCs and 10% SCs (Vijay et al., 2017). About 10-20% of the NCs, upon asymmetric division, will give rise to NCs and SCs, while the NCs and SCs by symmetric division will give rise to NCs and SCs, respectively (Vijay et al., 2017). However, the NCs and SCs, upon exposure to stress conditions such as antibiotics, oxidative or nitrite stress, will stop growth and division until they gain mutations, or upon removal of the stress, to re-grow and divide to give a normal mid-log phase population

consisting of 90% NCF cells and 10% SCF cells (Vijay et al., 2017; Nair et al., 2019a, b). However, what factors determine whether a mother cell will divide asymmetrically or symmetrically need further investigation.

Since SCs and NCs existed at the natural proportion of 1:9 (in terms of CFU) in the mid-log phase (MLP) cultures, we called the combined population of SCF and NCF reconstituted at 1:9 *in vitro*, as the **N**atural-**l**ike **P**roportion (**NLP**) (Fig. S1A, B). Whereas their combined population reconstituted *in vitro* at unnatural proportions (in terms of CFU) was called the Un-Natural Proportions (Fig. S1A, B). The total combined population containing all the Percoll fractions mixed back, as they existed in the MLP population, was termed the Total Reconstituted Population. The percentage survival in terms of CFUs of the NLP, Un-Natural Proportions, Total Reconstituted Population, and MLP population, against rifampicin, exogenously added H_2O_2, and isoniazid, was then determined in comparison to the survival of NCF which constituted ~90% of the population. Earlier, we had reported the different extents of survival of SCF and NCF over a wide range of concentrations of, and different durations of exposure to, rifampicin, isoniazid, and H_2O_2 (Vijay et al., 2017). From these observations, we selected the concentrations of rifampicin (25 μg ml^{-1}), isoniazid (2.5 μg ml^{-1}), and H_2O_2 (0.8 mM), which caused ~50% lethality to the subpopulations. This gave us reliable higher readout values of CFU for the comparative susceptibility of the different proportionate/unproportionate mixtures and NCF against the stress agents.

Catalase-peroxidase (KatG) degrades H_2O_2 and alleviates ROS invoked oxidative stress (Manca et al., 1999). Therefore, for studying the survival of the proportionate mixtures of the subpopulations against oxidative stress, we reconstituted NLPs with the SCF/NCF prepared from WT and *katG* or *furA-katG* knockout mutants (Δ*katG* or Δ*furA-katG*). Since dimethylthiourea (DMTU) is a H_2O_2 scavenger, we also used DMTU-exposed SCF (as a negative control). Thus, six types of NLP reagents were reconstituted *in vitro* at 1:9 proportion of: (i). WT-SCF with WT-NCF; (ii). WT-SCF(+)DMTU with WT-NCF(-)DMTU; and cross-mixtures of: (iii). Δ*furA-katG*-SCF with WT-NCF; (iv). WT-SCF with Δ*furA-katG*-NCF; (v). Δ*katG*-SCF with WT-NCF; and (vi). WT-SCF with Δ*katG*-NCF. Besides Δ*katG,* Δ*furA-katG* also was used since *furA* regulates *katG* expression in mycobacteria (Zahrt et al., 2001).

The use of the cell permeable H_2O_2 scavenger, DMTU (Jackson et al., 1985), was essential to scavenge the endogenous H_2O_2 generated inherently in SCs and NCs (Nair et al., 2019b). This would enable the incubation of DMTU-exposed SCF cells and its supernatant independently with the DMTU unexposed NCF cells prior to rifampicin exposure. The scavenging of endogenous H_2O_2 would not have been possible with the use of a cell impermeable H_2O_2 scavenger, such as catalase (Sylte et al., 2004). If the SCF cells or their supernatant was incubated with catalase, it would have scavenged the H_2O_2 released by the SCF cells but not the endogenous ROS.

Further, we did not use a *katG* overexpressing recombinant strain to demonstrate increased oxidative stress tolerance of the NCs. The reason was that *katG* overexpressing strain would express KatG in excess, either constitutively or upon induction of the strong promoter, unlike the naturally pulsed manner of *katG* expression in the wild type cells (Wakamoto et al., 2013). The high levels of KatG would not only scavenge the H_2O_2 generated inside the NCs during rifampicin exposure but will also scavenge the high levels of H_2O_2 inherently released by the SCs and permeating into the NCs. This condition may show a high oxidative stress survival in the *katG* overexpressing recombinant. However, it would not help to demonstrate the role of H_2O_2 released by SCs to enhance oxidative stress survival of NCs. Hence, we used the *furA-katG* and *katG* knockout strains. Using the percentage survival of NLPs, Un-Natural Proportions, Total Reconstituted Population, and MLP, against the oxidative stress invoked by rifampicin/H_2O_2 exposure, the mechanism of statistically significant enhancement of oxidative stress survival of NCF/NLP by the SCF in the NLP was elucidated. A model was proposed to depict the mechanism.

3.2. SCF enhanced the survival of NCF against rifampicin/H_2O_2

The percentage survival of NLP and their mean were always significantly higher than that of NCF upon exposure to rifampicin and H_2O_2 (Fig. S1A, B; Fig. 1A, B, and D; Fig. S2A, B for individual values; n = 10 biological replicates). Although the extent of percentage survival of NLP showed variations among the 10 biological replicates, in each NLP/NCF set, the percentage survival of NLP against rifampicin and H_2O_2 was always significantly higher than that of NCF. The significantly higher survival of NLP than NCF could be observed against a wide range of H_2O_2 concentrations and for different exposure durations (Fig. S3). In a few instances, the percentage survival of NLP against rifampicin/H_2O_2 exposure was >100%. This was due to the growth and division of the stress-tolerant cells during the stress exposure. Like NLP, MLP population that contained SCs and NCs at 1:9 proportion also showed significantly higher survival than NCF against the exogenously added H_2O_2 (Fig. S4). This close similarity in the survival of NLP and MLP validated the correctness of the composition of SCF and NCF in the *in vitro* reconstituted NLP. The significantly higher survival of NLP than NCF against H_2O_2 was like their higher survival against rifampicin reported by us earlier (Nair et al., 2019b). Similarly, the Total Reconstituted Population also showed significantly higher survival than NCF against H_2O_2 (Fig. S4), like their survival against rifampicin reported earlier (Nair et al., 2019b). The comparability of the mean percentage survival of NLP (fractionated and SCF/NCF reconstituted), MLP (unfractionated), and Total Reconstituted Population (fractionated and reconstituted with all the Percoll fractions proportionately) against H_2O_2 and rifampicin implied that Percoll or the Percoll fractionation process did not affect the response of these subpopulations to oxidative stress of rifampicin and H_2O_2.

3.3. Reduced survival of NLP against isoniazid and of Un-Natural Proportions

Contrary to the response to rifampicin and H_2O_2, NLP showed significant reduction in the percentage survival and their mean in comparison to that of NCF during exposure to isoniazid, a prodrug that requires catalase-peroxidase (KatG) mediated activation (Devi et al., 1975; Zhang et al., 1992) (Fig. 1C, D; and Fig. S2C; n = 10 biological replicates). This response could be observed at varied isoniazid concentrations and for different exposure durations (Fig. S5). Since higher KatG levels would result in the increased lethality to isoniazid (Zhang et al., 1992; Zhao et al., 2006), the higher susceptibility of NLP to isoniazid suggested the involvement of KatG in the survival of NCF/NLP. Since higher levels of KatG are induced by H_2O_2 (Master et al., 2001; Zhao et al., 2006; Voskuil et al., 2011; Li et al., 2015), NLP's decreased survival against isoniazid but not against rifampicin implied H_2O_2-mediated induction of KatG.

Unlike the higher survival of NLP, the Un-Natural Proportion 1, Un-Natural Proportion 2, and Un-Natural Proportion 3 that contained increasing proportions of SCF and correspondingly decreasing proportions of NCF, showed a sequential decrease in the mean percentage survival upon exposure to exogenously added H_2O_2 (Fig. S6). The decreased survival of the Un-Natural Proportions against H_2O_2 was like their decreased survival against rifampicin reported by us earlier (Nair et al., 2019b). Thus, in the Un-Natural Proportions, the steady increase in the proportion of the higher stress susceptible SCF (SCF1 and SCF2) with the proportionate reduction in the NCF indicated that the SCF was involved in the increased susceptibility of the Un-Natural Proportions.

3.4. Unstressed SCF's supernatant enhanced NCF's survival against rifampicin

The findings so far indicated that the co-existence of SCF at its natural proportion with NCF was necessary for its beneficial effect on NCF. This implied that the beneficial or detrimental effect, in terms of

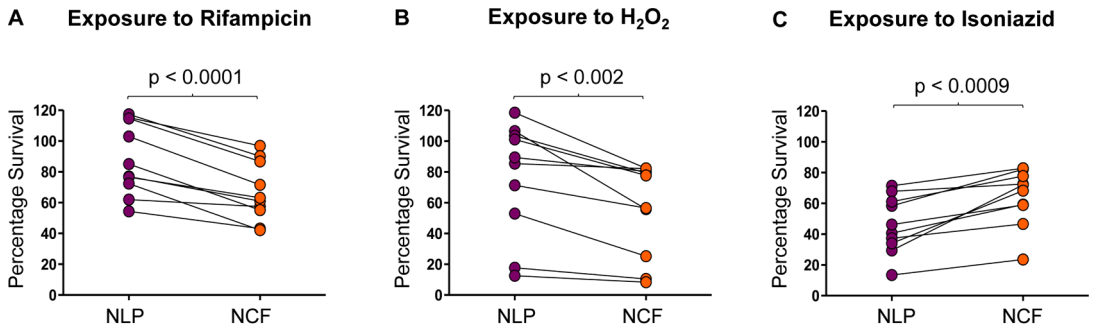

D

Stress Agent	Rifampicin		H_2O_2		Isoniazid	
Mean Percentage Survival	NLP	NCF	NLP	NCF	NLP	NCF
	87.71 ± 22.60	66.72 ± 18.67	75.89 ± 36.11	55.83 ± 29.51	46.01 ± 18.02	64.39 ± 17.81

Fig. 1. Percentage survival of the NLP and NCF cells exposed to rifampicin, H_2O_2, and isoniazid. Relative one-to-one correlation of the survival of the NLP and NCF cells in each independent set upon exposure to: (**A**) 25 μg/ml rifampicin; (**B**) 0.8 mM H_2O_2; and (**C**) 2.5 μg/ml isoniazid. (**D**) Mean percentage survival of the NLP and NCF cells upon exposure to the different stress agents. Their statistical significance was calculated using paired *t*-test (n = 10 biologically independent samples). **NLP**: **N**atural **L**ike **P**roportion; **NCF**: **N**ormal/long-sized **C**ells-enriched **F**raction.

enhanced or decreased survival of NCF, respectively, might have been mediated through inter-cellular communication or interaction of SCF with NCF. In agreement with this premise, the supernatant of the unstressed SCF (SCF1 & SCF2 combined) significantly increased the mean percentage survival of NCF against rifampicin to a level comparable to that of NLP (Fig. 2A). On the contrary, the supernatant of unstressed NCF did not change the mean percentage survival of either NCF or SCF against rifampicin (Fig. 2A and B, respectively). But the supernatant of the unstressed SCF significantly decreased the mean percentage survival of SCF itself against rifampicin (Fig. 2B). These observations indicated that some biomolecule from SCF present in its culture supernatant might have enhanced survival of NCF while being lethal to SCF itself during rifampicin exposure.

3.5. *H_2O_2 from SCF enhanced survival of NCF against rifampicin*

The survival of bacteria in the presence of antibiotics may facilitate the evolution of the generation of antibiotic resisters (Cohen et al., 2013; Sebastian et al., 2017; Swaminath et al., 2020; Hoeksema et al., 2018; Paul et al., 2021; Paul et al., 2022). We had earlier reported that the rifampicin resister generation frequency of NCF in the NLP was significantly enhanced by the H_2O_2 released from SCF into the culture supernatant (Nair et al., 2019b). Similarly, besides increasing the resister generation frequency of the NCF reported earlier (Nair et al., 2019b), the H_2O_2 naturally released from SCF increasing the survival of NCF against rifampicin was also a possibility. If this be the case, then the SCF exposed to non-lethal concentrations of the H_2O_2 scavenger, dimethyl thiourea (DMTU) (Parker et al., 1985) would not enhance the survival of NCF in

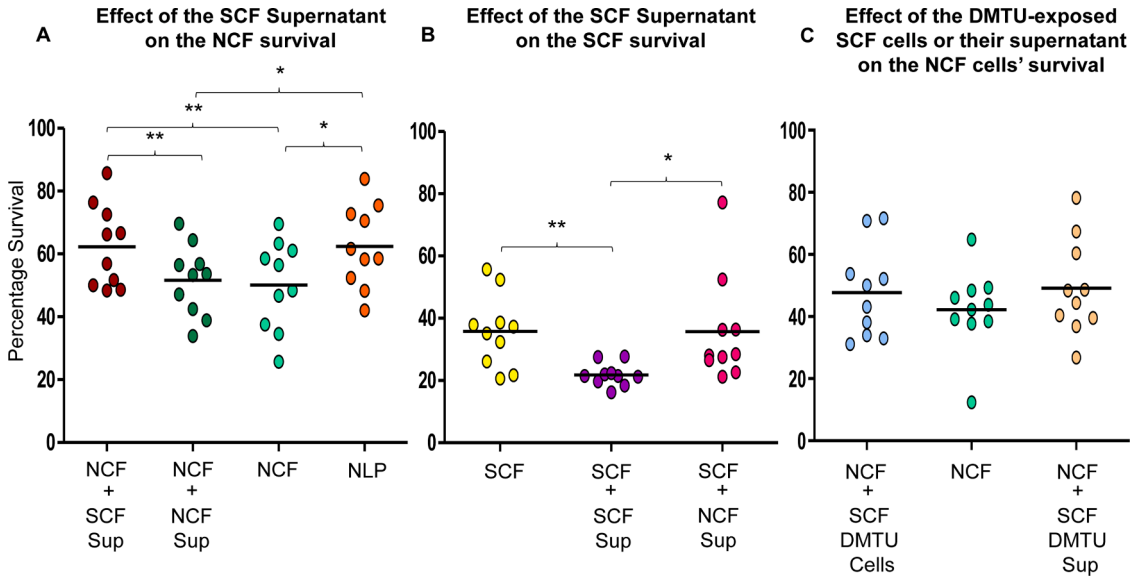

Fig. 2. Percentage survival of the NCF cells in the presence of the SCF/NCF supernatant during rifampicin exposure. Effect of the supernatant from the stress unexposed SCF and NCF cells on the survival of the: (**A**) NCF cells during rifampicin exposure; (**B**) SCF cells during rifampicin exposure; (**C**) Effect of the DMTU-exposed SCF cells or their supernatant on the survival of the NCF cells during rifampicin exposure. *, ** indicates $p \leq 0.05$ and $p \leq 0.01$, and the statistical significance was calculated using paired *t*-test (n = 10 biologically independent replicates).

the NLP against rifampicin. Similarly, the supernatant of the unstressed but DMTU-exposed SCF also would not enhance the survival of NCF in the NLP against rifampicin. Confirming these premises, the supernatant of the unstressed but DMTU-exposed SCF or the SCF from the MLP cultures grown in the continuous presence of DMTU could not significantly enhance the survival of NCF against rifampicin (Fig. 2C). Thus, it was the H_2O_2 naturally present in the SCF supernatant that enhanced the survival of NCF against rifampicin.

3.6. SCF induced katG in NCF/NLP

Among the different ROS, H_2O_2 has a half-life of 43.6 min in growth medium at neutral pH (Nakagawa et al., 2004). Although its permeability into bacterial cells is substantial but limited, it can passively diffuse across bacterial membranes (Seaver and Imlay, 2001). H_2O_2 is known to induce catalase-peroxidase (*katG*) (Master et al., 2001), the major enzyme that degrades H_2O_2 in mycobacteria (Manca et al., 1999). Therefore, it was likely that the H_2O_2 diffusing from SCF into the growth medium would have permeated into NCF and induced *katG* expression. The KatG in turn might have degraded the endogenous H_2O_2 formed as part of the oxidative stress invoked by rifampicin exposure (Nair et al., 2019a) or by the exogenously added H_2O_2 that permeated into NCF. This might have enhanced the survival of NCF against the oxidative stress caused by rifampicin/H_2O_2 exposure. We verified this possibility.

Of the three *katG* genes (*MSMEG_6384, MSMEG_3729*, and *MSMEG_3461*), *MSMEG_6384* is the only orthologue of *Mtb katG* in *Msm* (Iwao and Nakata, 2018). *MSMEG_6384* is also the major determinant of *Msm* susceptibility to isoniazid and to oxidative stress in the exponential growth phase (Iwao and Nakata, 2018). Hence to verify the involvement of *katG* (*MSMEG_6384*), we determined its mRNA levels in NCF and NLP, which were unexposed (0 min) or exposed for 2 min to rifampicin/H_2O_2. The *katG* mRNA levels were significantly higher in NLP as compared to NCF in the unexposed sample itself (Fig. 3A, B). Western blot analysis of 10 biological replicates also showed significant increase in KatG protein levels in the unexposed NLP (0 min), in comparison to NCF (Fig. 3C, D). The cytokinetic protein, FtsZ, the levels of which remain constant during cell cycle (Weart and Levin, 2003), was used as the loading control. Thus, KatG protein levels in the NCF existing in the unstressed MLP cultures was already naturally enhanced by the H_2O_2 inherently released by SCF. This, in turn, significantly increased NCF survival against rifampicin/H_2O_2 as compared to the stress susceptible SCF.

The exposure of NLP to rifampicin/H_2O_2 for 2 min decreased the levels of *katG* mRNA and protein (Fig. 3A, 3B and 3C, 3D, respectively). The *katG* transcription in mycobacteria is known to occur in pulses (Wakamoto et al., 2013). The decrease in the *katG* mRNA and protein levels could probably be due to the abrupt increase followed by a sudden decrease in the levels of *katG* mRNA, at the initiation and termination of this transcription pulse, respectively, as reported (Wakamoto et al., 2013). Variations in the KatG protein levels could be noted from experiment to experiment (Fig. 3D; n = 10 biological replicates), which would be reflective of the pulsed activity of the *katG* promoter reported (Wakamoto et al., 2013). Further, the variations in the KatG proteins levels might also be partly due to the utilisation of enhanced chemiluminescence method with HRP-conjugated secondary antibodies for the Western blot analysis. The results obtained using this method need not be consistent as the chemiluminescence depends on the substrate availability as well as the concentration of both HRP and the substrate (Pillai-Kastoori et al., 2020). Nevertheless, the variations in the *katG*

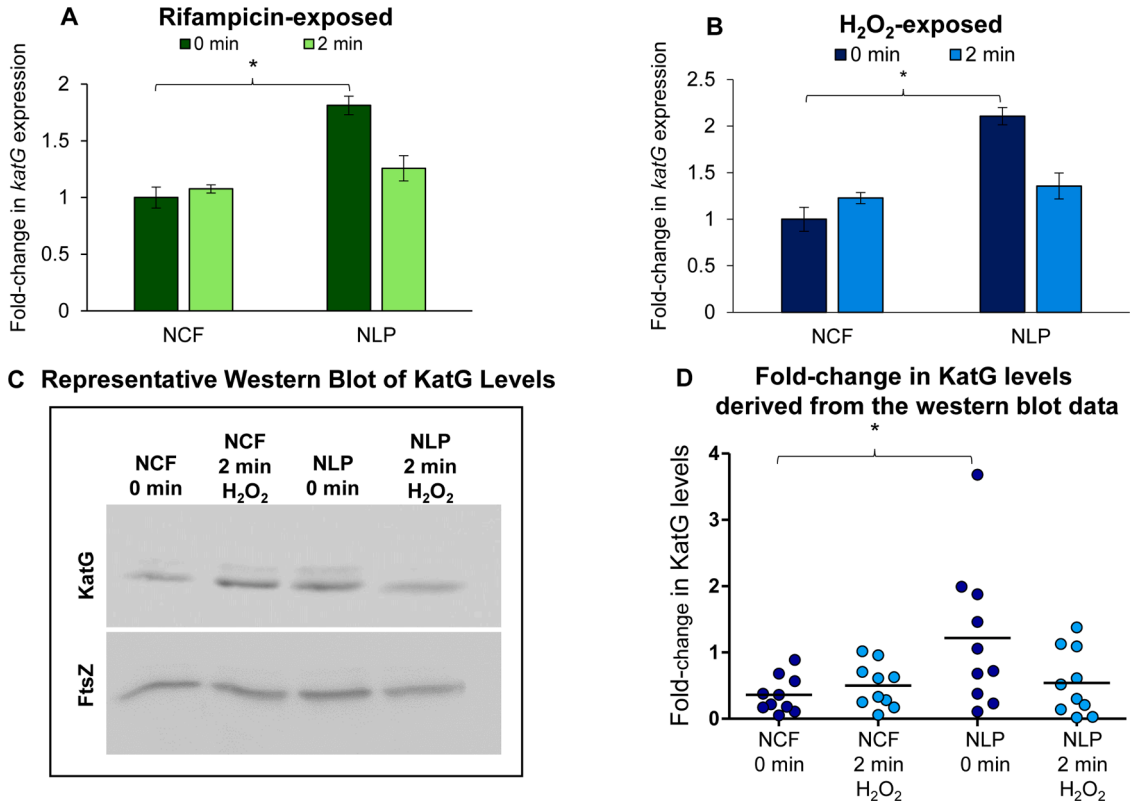

FIGURE 3. Fold-change in the *katG* mRNA and protein levels during exposure to rifampicin and H_2O_2. (**A, B**) Fold-change in the levels of *katG* mRNA in the NCF and NLP cells in the unexposed and 2 min exposed samples to: (**A**) rifampicin and (**B**) H_2O_2. Statistical significance was calculated using Student's *t*-test (n = 3 biological replicates). (**C**) Representative western blot profile of KatG levels in the unexposed and 2 min H_2O_2-exposed NCF and NLP cells, with FtsZ as the loading control. (**D**) Fold-change in the levels of KatG in the unexposed and 2 min H_2O_2-exposed NCF and NLP cells, derived from the western blot data of 10 independent samples, with a representative profile shown in (**C**). * indicates $p \leq 0.05$, and the statistical significance was calculated using paired *t*-test (n = 10 biologically independent replicates).

mRNA levels determined at every one min interval for 15 min in the biological triplicate samples of NLP and NCF exposed to 0.8 mM H_2O_2 confirmed the pulsed activity of *katG* promoter (Fig. S7A-C). Despite these variations, the NLP samples most often showed higher levels of *katG* mRNA than the respective NCF samples. This is probably due to the *katG* transcription priming by the H_2O_2, released by the SCF cells, in the NLP. These findings indicated that the increased *katG* expression in the NCF cells of NLP, facilitating their enhanced survival against oxidative stress, would have been already primed by the H_2O_2 naturally released by the SCF component in the NLP mixture in the unstressed actively growing condition itself.

3.7. The H_2O_2 from SCF induced katG in NCF/NLP

The *katG* mRNA levels in NCF were found to increase significantly upon addition of the supernatant from the unstressed SCF (Fig. 4A). This strengthened the possibility that the H_2O_2 released by SCF would have induced significantly high levels of *katG* in the NCF of NLP, as compared to NCF alone. On the contrary, the supernatant of the SCF isolated from the MLP culture grown in the presence of DMTU (H_2O_2 scavenger) (Parker et al., 1985), did not increase *katG* mRNA levels in NCF (Fig. 4A). Since H_2O_2 increases *katG* transcription in mycobacteria (Master et al., 2001), we wanted to find out whether the increase in the *katG* mRNA levels in NCF was due to transcriptional increase induced by the H_2O_2 inherently released by the unstressed SCF.

For this purpose, we generated *Msm*/pAKMN2-*PfurA-katG-ugfp*$_m^{2+}$ genome-integrant strain carrying transcriptional fusion of the *furA-katG* promoter to the mycobacterial codon-optimised unstable *gfp*$_m^{2+}$ (*ugfp*$_m^{2+}$) integrated at the L5 mycobacteriophage *att* site in the genome as a single copy (Roy et al., 2012; Sebastian, 2016). The expression levels of *katG* and *ugfp*$_m^{2+}$ mRNAs in this strain were determined using RT-qPCR in NCF and NLP prepared from the MLP cultures of *Msm*/pAKMN2-*PfurA-katG-ugfp*$_m^{2+}$ strain. In the NLP, reconstituted with the integrant SCF and NCF, the endogenous *katG* mRNA expression levels were found to be significantly higher, as compared to the levels in the integrant NCF alone (Fig. 4B). But in the NCF cells of the NLP, reconstituted with NCF and SCF prepared from the *Msm* integrant strain cultured in the presence of DMTU, the *katG* mRNA levels did not show increase (Fig. 4B). It confirmed that the H_2O_2 released by SCF into the supernatant, which was reported by us earlier (Nair et al., 2019b), enhanced the *katG* levels in the NCF in the NLP mixture.

Like the *katG* mRNA levels, the levels of expression of the reporter *ugfp*$_m^{2+}$ mRNA driven by the *furA-katG* promoter, were also found to be significantly higher in NLP, as compared to the levels in NCF (Fig. 4C). The integrant NLP, which was reconstituted with NCF and the DMTU-exposed SCF, did not show enhanced levels of *ugfp*$_m^{2+}$ mRNA (Fig. 4C). These experiments showed that the *katG/ugfp*$_m^{2+}$ mRNA was expressed by the NCF in the NLP in response to the H_2O_2 released by the SCF in the NLP. The comparable fold-change in the expression levels of *ugfp*$_m^{2+}$ and *katG* in NCF and NLP (Fig. 4B, C), validated the aptness of the usage of the integrant strain.

In correlation with the significant increase in the *katG/ugfp*$_m^{2+}$ mRNA levels determined using RT-qPCR, flow cytometry analysis showed a significant increase in the uGFP$_m^{2+}$ protein fluorescence in the NLP reconstituted with NCF/pAKMN2-*PfurA-katG-ugfp*$_m^{2+}$ and WT-SCF (Fig. 4D). On the contrary, the NCF/pAKMN2-*PfurA-katG-ugfp*$_m^{2+}$ alone or the NLP reconstituted with NCF/pAKMN2-*PfurA-katG-ugfp*$_m^{2+}$ and DMTU-exposed WT-SCF did not show enhanced uGFP$_m^{2+}$ protein fluorescence (Fig. 4D). These observations confirmed that the increase in the *katG mRNA*/protein levels was brought about by the transcriptional induction of the *PfurA-katG* promoter of the NCF in the NLP by the H_2O_2 released by the SCF.

3.8. Increased KatG levels enhanced NLP cells' survival against rifampicin/H_2O_2

The involvement of KatG in the enhanced survival of NLP was confirmed using the Δ*furA-katG* and Δ*katG* NLP cells, which were prepared from the Δ*furA-katG* and Δ*katG* NCF and SCF. The Δ*furA-katG* NLP showed significantly less survival, as compared to the Δ*furA-katG* NCF alone against rifampicin (Fig. 5A, C; Fig. S8A gives actual values) and H_2O_2 (Fig. 5D, F; Fig. S8C gives actual values). On the contrary, the NLP reconstituted with WT-NCF and WT-SCF showed significant increase in the survival against rifampicin (Fig. 5B, C; Fig. S8B) and H_2O_2 (Fig. 5E, F; Fig. S8D). Similarly, Δ*katG* NLP also showed significantly reduced survival than Δ*katG* NCF against rifampicin (Fig. 6A, C; Fig. S9A) and H_2O_2 (Fig. 6D, F; Fig. S9C). Here also, the NLP reconstituted with WT-NCF and WT-SCF showed significant increase in the survival against rifampicin (Fig. 6B, C; Fig. S9B) and H_2O_2 (Fig. 6E, F; Fig. S9D). Thus, the higher susceptibility of Δ*furA-katG* / Δ*katG* NLP, as compared to the Δ*furA-katG* / Δ*katG* NCF, would be due to the H_2O_2 released by the Δ*furA-katG* / Δ*katG* SCF permeating into the Δ*furA-katG*

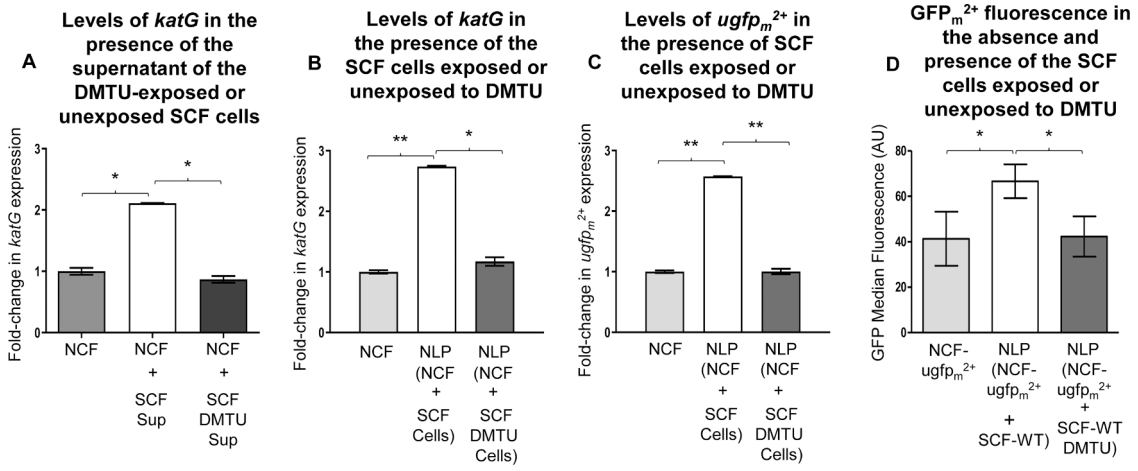

Fig. 4. Fold-change in the levels of the native *katG* mRNA and of the *katG* promoter driven *ugfp*$_m^{2+}$ mRNA in the NCF cells in the presence of DMTU-exposed/unexposed SCF cells or their supernatant. (**A-C**) RT-qPCR analysis of: (**A**) *katG* mRNA levels in the NCF cells in the presence of the supernatant from the stress-unexposed and DMTU-exposed SCF cells; (**B**) *katG* mRNA levels in the NCF cells in the presence of stress-unexposed and DMTU-exposed SCF cells (prepared from *Msm/PfurA-katG-ugfp*$_m^{2+}$ genome integrant); (**C**) *ugfp*$_m^{2+}$ reporter mRNA levels in the NCF cells in the presence of stress-unexposed and DMTU-exposed SCF cells (prepared from *Msm/PfurA-katG-ugfp*$_m^{2+}$ genome integrant). (**D**) Flow cytometry quantitation of GFP$_m^{2+}$ fluorescence in the *Msm/PfurA-katG-ugfp*$_m^{2+}$ genome integrated NCF cells in the presence of stress-unexposed and DMTU-exposed SCF-WT cells. *, ** indicates $p \leq 0.05$ and $p \leq 0.01$, and the statistical significance was calculated using Students' *t*-test (n = 3 biologically independent replicates).

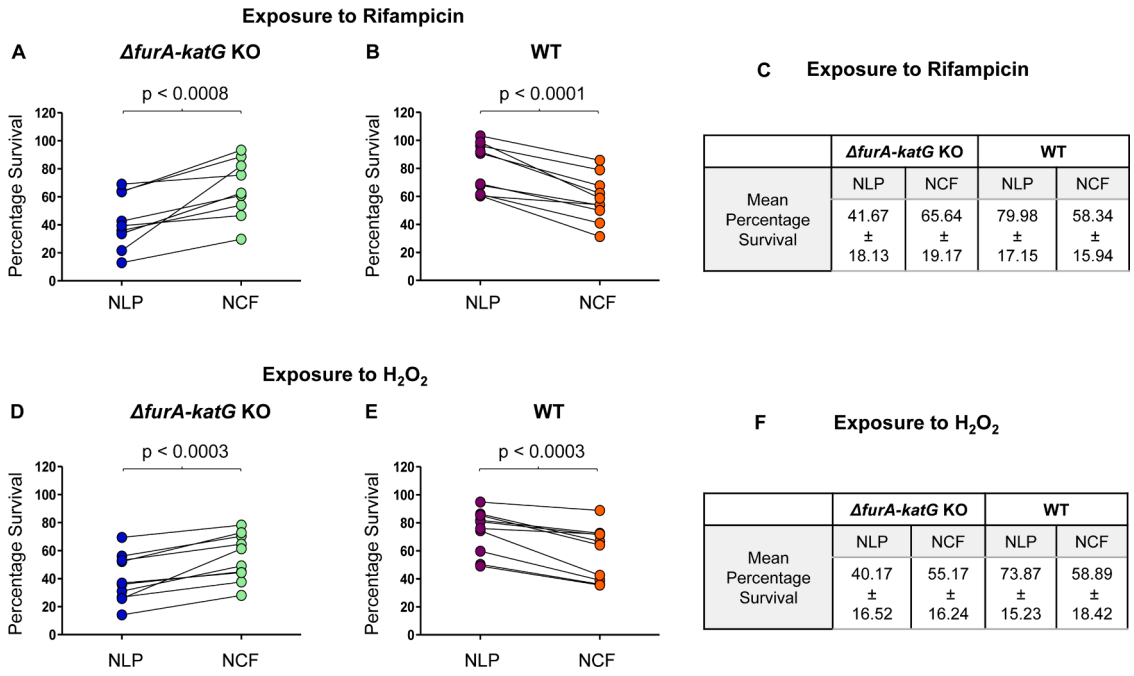

	ΔfurA-katG KO		WT	
	NLP	NCF	NLP	NCF
Mean Percentage Survival	41.67 ± 18.13	65.64 ± 19.17	79.98 ± 17.15	58.34 ± 15.94

	ΔfurA-katG KO		WT	
	NLP	NCF	NLP	NCF
Mean Percentage Survival	40.17 ± 16.52	55.17 ± 16.24	73.87 ± 15.23	58.89 ± 18.42

Fig. 5. Percentage survival of the WT and Δ*furA-katG* KO mutant upon exposure to rifampicin and H_2O_2. (**A, B**) Relative one-to-one correlation of the survival of the rifampicin-exposed NLP and NCF cells in each independent set: (**A**) Δ*furA-katG* KO and (**B**) WT. (**D, E**) Relative one-to-one correlation of the survival of the H_2O_2-exposed NLP and NCF cells in each independent set: (**D**) Δ*furA-katG* KO and (**E**) WT. Mean percentage survival of the KO and WT strains of NLP and NCF when exposed to: (**C**) rifampicin and (**F**) H_2O_2 with their statistical significance calculated using paired *t*-test (n = 10 biologically independent samples).

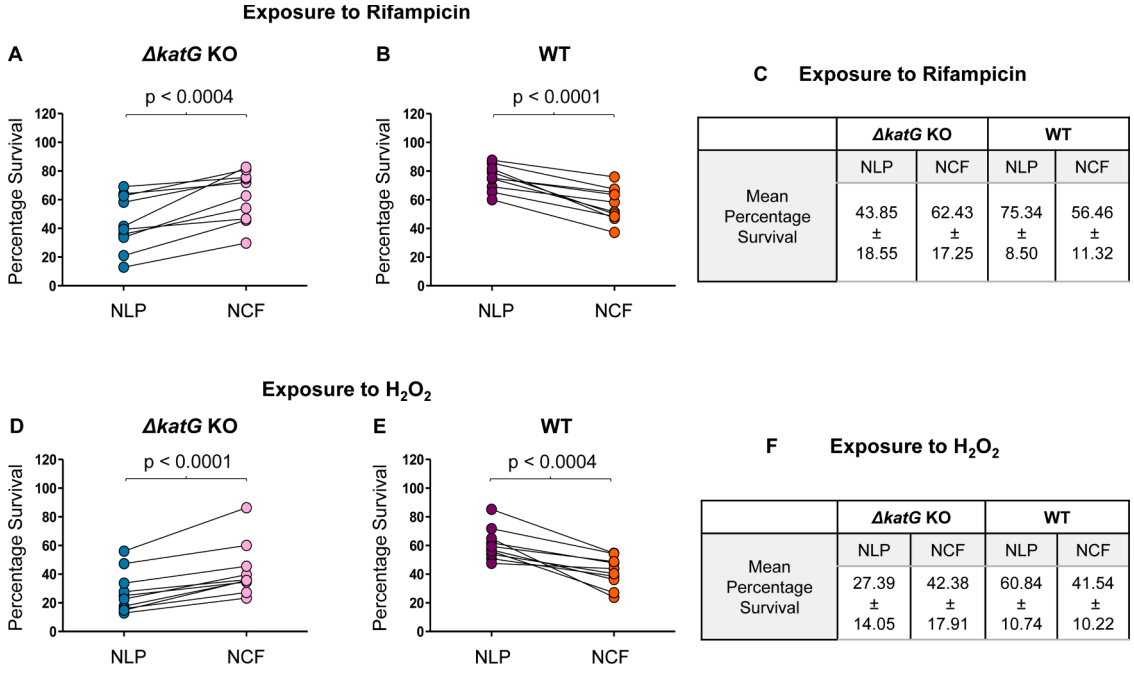

	ΔkatG KO		WT	
	NLP	NCF	NLP	NCF
Mean Percentage Survival	43.85 ± 18.55	62.43 ± 17.25	75.34 ± 8.50	56.46 ± 11.32

	ΔkatG KO		WT	
	NLP	NCF	NLP	NCF
Mean Percentage Survival	27.39 ± 14.05	42.38 ± 17.91	60.84 ± 10.74	41.54 ± 10.22

Fig. 6. Percentage survival of the WT and Δ*katG* KO mutant during exposure to rifampicin and H_2O_2. (**A, B**) Relative one-to-one correlation of the survival of the rifampicin-exposed NLP and NCF cells in each independent set: (**A**) Δ*katG* KO and (**B**) WT. (**D, E**) Relative one-to-one correlation of the survival of the H_2O_2-exposed NLP and NCF cells in each independent set: (**D**) Δ*katG* KO and (**E**) WT. Mean percentage survival of the KO and WT strains of NLP and NCF when exposed to: (**C**) rifampicin and (**F**) H_2O_2. The statistical significance was calculated using paired *t*-test (n = 10 biologically independent samples).

/ Δ*katG* NCF (in the Δ*furA-katG* / Δ*katG* NLP) and remaining unneutralised due to the absence of KatG in Δ*furA-katG* / Δ*katG* NCFs. Whereas, in the absence of the H_2O_2 releasing Δ*furA-katG* / Δ*katG* SCF, the Δ*furA-katG* / Δ*katG* NCFs incubated alone survived better as they were not exposed to H_2O_2.

Like in the case of the significantly higher survival of WT-NCF than the WT-SCF against rifampicin/H_2O_2, the Δ*furA-katG* / Δ*katG* NCF also showed significantly higher survival than the respective Δ*furA-katG* / Δ*katG* SCF1 and Δ*furA-katG* / Δ*katG* SCF2 (Fig. S10 and Fig. S11). Thus, the significantly higher survival of NCF than SCF, despite whether they were WT or Δ*furA-katG* / Δ*katG*, showed that NCF was the stress survived subpopulation. Further, the significantly reduced survival of the

Δ*furA-katG* / Δ*katG* NLP than their respective WT NCF cells indicated that the *katG* of NCF was required for the enhanced survival of NLP. It indicated that *katG* of NCF would be involved in mediating the oxidative stress survival of NCF in the NLP. These observations established that the high *katG* levels induced in NCF by SCF in NLP mixture would have enhanced the survival of NCF, and thereby the survival of NLP, against rifampicin and H_2O_2. Since isoniazid requires KatG mediated activation (Devi et al., 1975; Zhang et al., 1992), the extent of survival of Δ*furA-katG* / Δ*katG* NCF and NLP against isoniazid was not determined.

3.9. NLP cross-mixtures of WT & KO confirmed KatG of NCF the mediator, SCF the H_2O_2 donor, and NCF the enhanced survival beneficiary

To confirm that it is the increase in the KatG levels in the NCF in NLP that conferred the enhanced survival against rifampicin/H_2O_2, NLP cross-mixtures containing NCF and SCF of WT and Δ*furA-katG* or Δ*katG* strains were prepared. These NLPs were: (i). WT-SCF with Δ*furA-katG*-KO-NCF; (ii). WT-SCF with Δ*katG*-KO-NCF; (iii). Δ*furA-katG*-KO-SCF with WT-NCF; and (iv). Δ*katG*-KO-SCF with WT-NCF. The NLP cross-mixtures of Δ*furA-katG*-KO-SCF with WT-NCF or Δ*katG*-KO-SCF with WT-NCF showed significantly enhanced survival as compared to WT-NCF against rifampicin (Fig. 7A, C; Fig. S12A; Fig. 8A, C; Fig. S13A, respectively) and H_2O_2 (Fig. 7D and F; Fig. S12C; Fig. 8D and F; Fig. S13C, respectively). On the contrary, the NLP cross-mixtures of WT-SCF with Δ*furA-katG*-KO-NCF or WT-SCF with Δ*katG*-KO-NCF showed a significant reduction in the survival as compared to Δ*furA-katG*-KO-NCF or Δ*katG*-KO-NCF against rifampicin (Fig. 7B and C; Fig. S12B; Fig. 8B and C; Fig. S13B, respectively) and H_2O_2 (Fig. 7E and F; Fig. S12D; Fig. 8E and F; Fig. S13D, respectively). Since WT-SCF naturally releases significantly higher quantity of H_2O_2 than WT-NCF (Nair et al., 2019a, b), the decreased survival of the NLP cross-mixtures of WT-SCF with Δ*furA-katG*-KO-NCF or WT-SCF with Δ*katG*-KO-NCF, as compared to Δ*furA-katG*-KO-NCF or Δ*katG*-KO-NCF alone, would be due to the H_2O_2 toxicity from WT-SCF on the KatG-lacking Δ*furA-katG*-KO-NCF or Δ*katG*-KO-NCF. On the contrary, the NLP cross-mixtures of Δ*furA-katG*-KO-SCF with WT-NCF or Δ*katG*-KO-SCF with WT-NCF showed enhanced survival. Thus, these results confirmed that it was: (i) the KatG of NCF that aided the enhanced survival of NLP against rifampicin/H_2O_2, and (ii) the H_2O_2 released by the SCF in the NLP mixture induced *katG* in the NCF, which in turn enhanced survival of the NCF against rifampicin/H_2O_2. The enhanced survival of NLP was due to the enhanced survival of NCF in the NLP. Thus, SCF is the natural benefactor and NCF is the natural beneficiary in the phenomenon of enhanced survival of the NLP cells. These observations showed that the natural presence of SCF and NCF at 1:9 proportion in the NLP/MLP/Total Reconstituted Population populations kept NCF already inherently and naturally primed by the SCF-H_2O_2 cross-inducing KatG in NCF to face oxidative stress whenever exposed to rifampicin/H_2O_2.

3.10. The quantity and implications of the H_2O_2 released by SCF

The expression of *katG* in mycobacteria has been found to be induced by different concentrations of H_2O_2 (Voskuil et al., 2011; Li et al., 2015). The expression pattern of *katG* was found to increase steadily from 2.1-fold to 12-fold upon exposure of *Mtb* cells to 0.05-10 mM H_2O_2 for 40 min (Voskuil et al., 2011). However, a drastic decrease in the *katG* expression was observed when exposed to 50 mM H_2O_2, probably owing to the collapse of the transcriptional machinery in the stress susceptible cells (Voskuil et al., 2011). Further, since the expression of *katG* was found to increase by 2.1-fold upon exposure of 10^7 cells ml^{-1} to 0.05 mM H_2O_2, it could be inferred that each cell was exposed to 5×10^{-9} μmoles of H_2O_2 that induced *katG* expression in *Mtb* (Voskuil et al., 2011). Similarly, the *katG* expression was found to increase by 12-fold upon exposure of ~0.5×10^8 cells ml^{-1} to 0.2 mM H_2O_2 for 30 min in *Msm*,

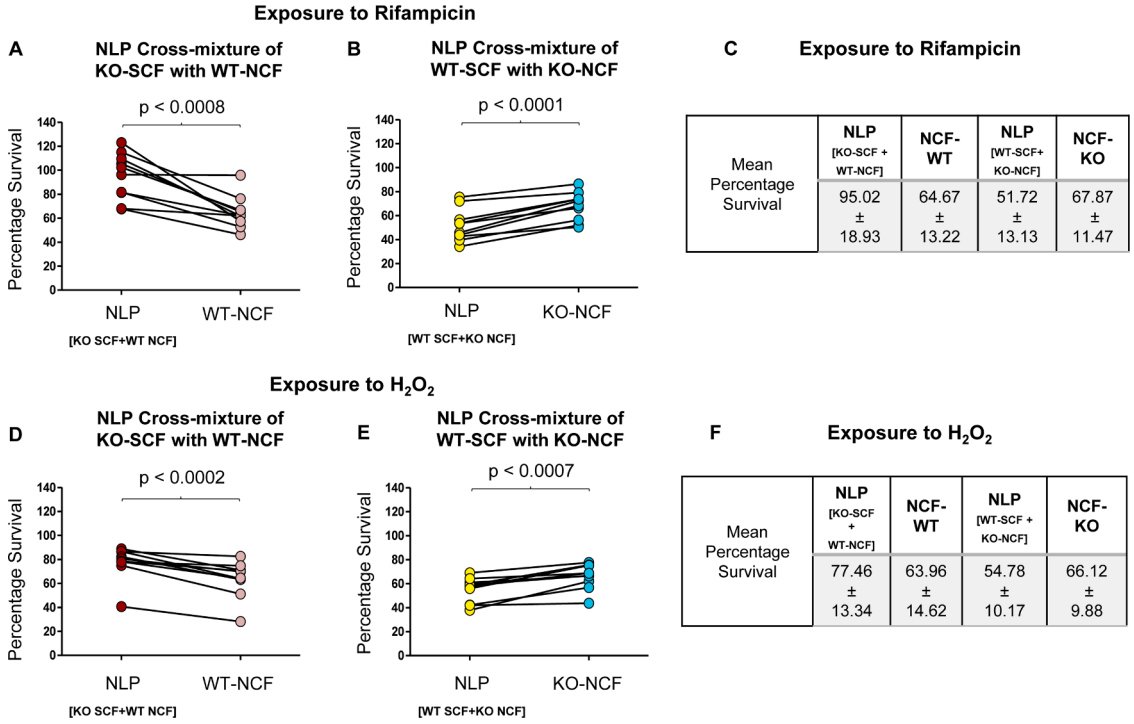

	NLP [KO-SCF + WT-NCF]	NCF-WT	NLP [WT-SCF+ KO-NCF]	NCF-KO
Mean Percentage Survival	95.02 ± 18.93	64.67 ± 13.22	51.72 ± 13.13	67.87 ± 11.47

	NLP [KO-SCF + WT-NCF]	NCF-WT	NLP [WT-SCF + KO-NCF]	NCF-KO
Mean Percentage Survival	77.46 ± 13.34	63.96 ± 14.62	54.78 ± 10.17	66.12 ± 9.88

Fig. 7. Percentage survival of the cross-mixtures of the WT and Δ*furA-katG* KO strains exposed to rifampicin and H_2O_2. (**A, B**) Relative one-to-one correlation of the survival of the rifampicin-exposed: (**A**) NLP cells (containing KO-SCF and WT-NCF) and WT-NCF cells; (**B**) NLP cells (containing WT-SCF and KO-NCF) and KO-NCF cells, in each independent set. (**D, E**) Relative one-to-one correlation of the survival of the H_2O_2-exposed: (**D**) NLP cells (containing KO-SCF and WT-NCF) and WT-NCF cells; (**E**) NLP cells (containing WT-SCF and KO-NCF) and KO-NCF cells, in each independent set. Mean percentage survival of the cross-mixtures with their respective NCF cells when exposed to (**C**) rifampicin and (**F**) H_2O_2. The statistical significance was calculated using paired *t*-test (n = 10 biologically independent samples).

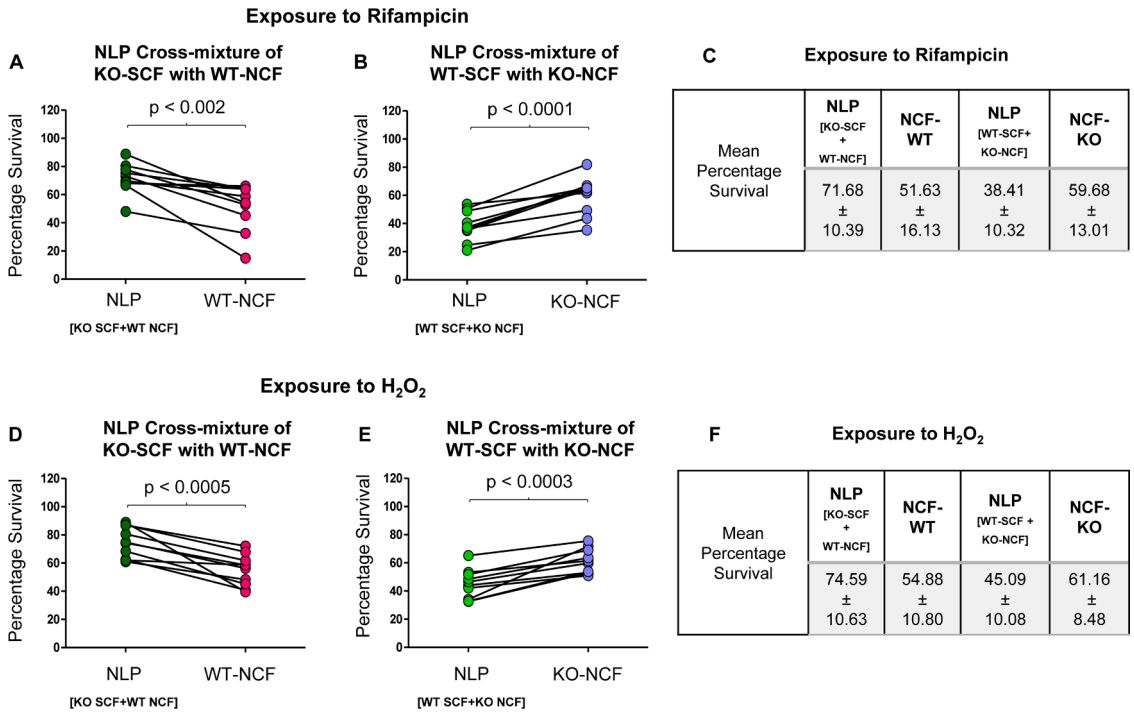

Fig. 8. Percentage survival of the cross-mixtures of the WT and Δ*katG* KO strains exposed to rifampicin and H_2O_2. (**A, B**) Relative one-to-one correlation of the survival of the rifampicin-exposed: (**A**) NLP cells (containing KO-SCF and WT-NCF) and WT-NCF cells; (**B**) NLP cells (containing WT-SCF and KO-NCF) and KO-NCF cells, in each independent set. (**D, E**) Relative one-to-one correlation of the survival of the H_2O_2-exposed: (**D**) NLP cells (containing KO-SCF and WT-NCF) and WT-NCF cells; (**E**) NLP cells (containing WT-SCF and KO-NCF) and KO-NCF cells, in each independent set. Mean percentage survival of the cross-mixtures with their respective NCF cells when exposed to (**C**) rifampicin and (**F**) H_2O_2. The statistical significance was calculated using paired *t*-test (n = 10 biologically independent samples).

which amounted to 4×10^{-9} μmoles of H_2O_2 per cell exposed (Li et al., 2015).

In the background of these findings, in the present study, significant induction of *katG* was found in the NCF due to the high levels of H_2O_2 inherently released by the unstressed SCF in the actively growing MLP cultures. We had earlier reported that the SCF inherently released $2.977 \pm 0.30 \times 10^{-10}$ μmoles of H_2O_2 per cell (Nair et al., 2019b). From the CFU of the SCF and NCF constituting NLP, we determined the number of SCF cells to be $64.75 \pm 93.33 \times 10^3$ cells ml^{-1} and that of NCF cells to be $1028.91 \pm 882.77 \times 10^3$ cells ml^{-1} in the NLP (calculated from 10 independent biological samples; n = 10). The following calculations are given under '**Supplementary Text on H_2O_2 Levels per Cell**' in the Supplementary Material. The SCF cells in the NLP, present in 25 ml Middlebrook 7H9 medium, would release $4.82 \pm 6.95 \times 10^{-4}$ μmoles of H_2O_2 ($25 \times 64.75 \pm 93.33 \times 10^3$ x 2.977×10^{-10}). Further, the $2.57 \pm 2.21 \times 10^7$ NCF cells ($1028.91 \pm 882.77 \times 10^3$ x 25) present in 25 ml of the medium will be exposed to $4.82 \pm 6.95 \times 10^{-4}$ μmoles of H_2O_2. Thus, each NCF cell would be exposed to $1.97 \pm 1.76 \times 10^{-11}$ μmoles of H_2O_2 ($4.82 \pm 6.95 \times 10^{-4} \div 2.57 \pm 2.21 \times 10^7$) that naturally induced *katG* expression (~2-fold) in the NCF cells, which primed the NCF cells for enhanced survival against the oxidative stress induced by rifampicin and exogenously added H_2O_2. However, exogenous addition of 0.8 mM H_2O_2 into the culture would result in an exposure of $2.08 \pm 1.47 \times 10^{-6}$ μmoles of H_2O_2 per cell, which would be more lethal for the NCF cells when present alone. But in the MLP/NLP/Total Reconstituted Population cultures, where the SCF cells co-exist with the NCF cells at the natural 1:9 ratio, the *katG* induced in the NCF cells by the H_2O_2 released inherently by the SCF cells enhanced survival of the NCF cells against the oxidative stress induced by rifampicin/H_2O_2 exposure. Thus, the NCF cells were ready to face oxidative stress with the already expressed KatG which could neutralise the endogenous H_2O_2 formation caused by the exposure to rifampicin/exogenous H_2O_2.

3.11. The mechanism of NCF's enhanced survival mediated by SCF's H_2O_2

The current study revealed a unique mechanism by which a minor subpopulation, the SCs (SCF cells), aided in enhancing the survival of the major kin subpopulation, the NCs (NCF cells), against rifampicin and H_2O_2, in the mycobacterial MLP cultures. The survival was brought about by a neutralisation mechanism of the oxidative stress generated by the two stress agents by an inherent feature of the unstressed SCs. The features of the inherent differential survival mechanism of SCs and NCs against oxidative stress revealed by the study are: (i). the native unstressed minor subpopulation, the SCs, inherently released significantly high levels of H_2O_2; (ii). the released H_2O_2 present in the medium induced significantly high levels of *katG* expression in NCs; (iii). the significantly high KatG protein levels induced in NCs in the unstressed whole population degraded the endogenous H_2O_2 formed in response to rifampicin, resulting in their enhanced survival; (iv). the survival enhancement against rifampicin occurred only in the: (a) natural MLP population, (b) *in vitro* reconstituted Total Reconstituted Population that was like MLP population, and (c) *in vitro* reconstituted NLP containing SCs and NCs at 1:9, but not at unnatural proportions. The unique and novel aspect of the phenomenon of survival enhancement of NCs by SCs was that the unstressed NCs in the actively growing *Msm* cultures were already primed by SCs to neutralise oxidative stress whenever generated by stress agents. These features are depicted in a model (Fig. 9).

4. Discussion

4.1. Differential generation of H_2O_2 by SCs/NCs enabled oxidative stress survival

The present findings stand as a unique example of how the significant differential generation of H_2O_2 between two bacterial subpopulations

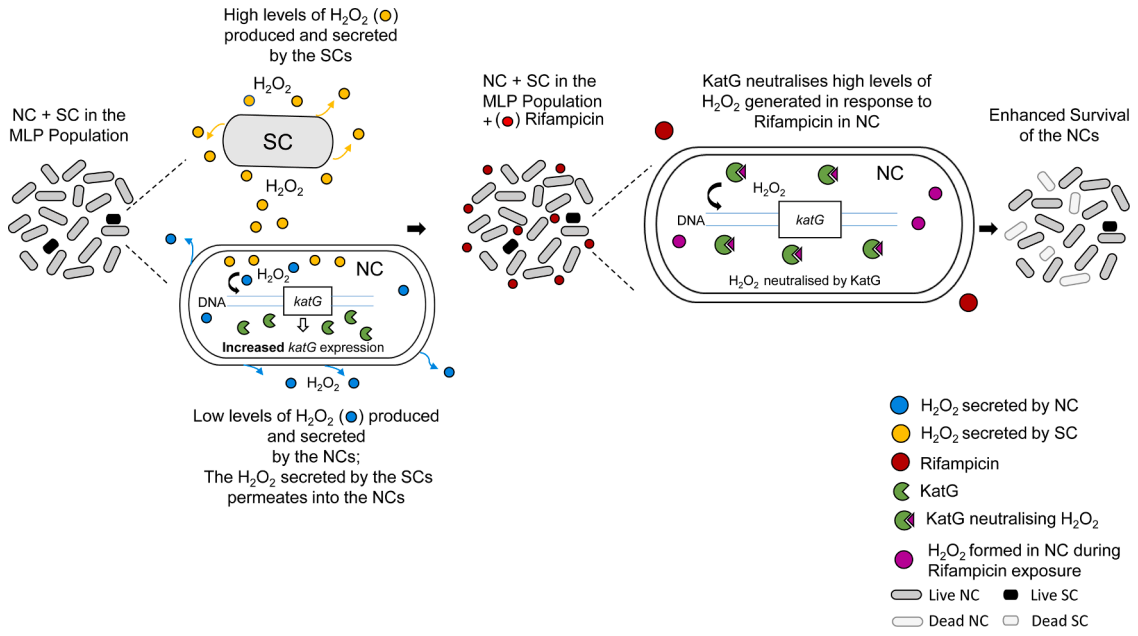

Fig. 9. Model depicting the SCs priming the NCs to enhance their survival against the endogenous H_2O_2 generated in response to rifampicin. The SCs release high levels of H_2O_2 which significantly increase *katG* expression in the NCs co-existing with the SCs at 9:1 ratio in the MLP population. Upon exposure to rifampicin, the H_2O_2 generated in the NCs in response to rifampicin gets neutralised by the KatG resulting in the enhanced survival of the NCs against rifampicin. The SCs and the NCs are not drawn to the 1:9 proportion indicated in the data due to space constraints.

enabled their survival against oxidative stress. We recently showed that the inherently high levels of generation of H_2O_2 by the SCs was due to the high levels of expression of NADH oxidase generating significantly elevated levels of superoxide (Nair et al., 2019b). The high levels of superoxide produced H_2O_2 and eventually resulted in the formation of hydroxyl radical at significantly elevated levels. The high levels of hydroxyl radical inflicted genome-wide mutations thereby increasing antibiotic resister generation frequency of SCs despite their inherently higher susceptibility to oxidative stress. The present study has further advanced this finding to demonstrate the mechanism of how the significant differential generation of H_2O_2 conferred the additional benefit of enhanced survival of NCs also against the oxidative stress imposed by rifampicin/H_2O_2. Thus, the high levels of H_2O_2 produced inherently by a minor subpopulation eventually ensured the survival of both the minor and the major kin subpopulations against rifampicin-invoked oxidative stress. This was achieved through two different modes of utilisation of the same ROS, H_2O_2, one by enhancing the survival of NCs and the other by enhancing the rifampicin resister generation frequency of SCs. Hence, by the effective employment of a single ROS, the survival of both the subpopulations was ensured. Thus, the mechanisms that made the two subpopulations produce differential levels of H_2O_2 have significance in the evolution of antibiotic resistance.

In a similar instance, as a survival strategy against nutritional stress, nutrient upshift of starved *E. coli* cells caused the emergence of partially metabolically active cells, which spontaneously restored their metabolism upon long-term incubation (Şimşek and Kim, 2018). Another example of cellular differences driven differential survival is that of a subpopulation of the fungus, *Cryptococcus gattii*, which when confronted with the host ROS, attained tubular mitochondrial morphology that promoted growth of the neighboring cells with non-tubular mitochondrial morphology, thereby helping the pathogen to establish infection in the host (Voelz et al., 2014).

4.2. The relevance of 1:9 SCs:NCs ratio in oxidative stress survival

It was the natural 1:9 proportion of the SCs:NCs at which the significantly high levels of H_2O_2 inherently released by the 10% proportion of the SCs became stoichiometrically beneficial to the 90% proportion of the NCs, despite remaining lethal to the SCs upon rifampicin exposure. The occurrence of the enhanced survival phenomenon over a wide range of exogenously added H_2O_2 concentrations (see **Fig. S3**) ascertained the robustness of the response of the bacilli to survive against wide variations in the concentrations of the oxidative stress agent. This would as well hold true in the survival against oxidative stress invoked by wide range of rifampicin concentrations. Further, the high H_2O_2 levels being deleterious, for the population's survival it was only logical that the minor subpopulation, and not the major subpopulation, evolved the ability to produce and release significantly more H_2O_2. Even though the production of high levels of H_2O_2 inflicted higher stress susceptibility, it ironically conferred the benefit of significantly higher resister generation frequency (Nair et al., 2019b).

4.3. The continuous priming of KatG levels for oxidative stress survival

Our present study has elucidated the mechanism behind the earlier report from another group on the naturally high KatG levels continuously priming *M. tuberculosis* to face oxidative stress (Voskuil et al., 2011). The naturally high levels of KatG in the *M. tuberculosis* whole population observed by them would have been mainly due to the SCs-released H_2O_2-mediated continuous induction of *katG* occurring in the NCs in the MLP populations. Since NCs constituted 90% of the population (Vijay et al., 2014a), the higher levels of KatG detected in the whole population (Voskuil et al., 2011) would have been from the NCs. Since SCs continuously prime NCs to produce higher levels of KatG, NCs would always contain high KatG levels. However, in the present study, at the 0 min (unstressed condition), the KatG levels in NCF cells (obtained after 1 hr of Percoll gradient centrifugation) were low (see Fig. 3C). This could have been probably due to the short half-life of KatG in *Msm* (0.7 hrs) (Wakamoto et al., 2013) that would have caused the decline in the H_2O_2 levels during the enrichment process. Thus, the higher levels of KatG, which might have been originally present in the NCs, would have got reduced during the enrichment of NCs/SCs that lasted for an hour. Thus, the reduced KatG levels would have got significantly increased by the H_2O_2 released by the unstressed SCF cells (see Fig. 4A, B). In fact, it was a matter of serendipity that the one-hour long enrichment process for NCs/SCs enabled demonstration of the

enhancement of KatG levels in NCs. We could not determine the KatG protein levels in SCs due to the very low cell density. Due to the stochastic nature of H_2O_2 production by SCs (Nair et al., 2019b), we did not attempt estimation of KatG levels by pooling multiple SCF preparations. The significantly high levels of *katG* mRNA in SCF found earlier would have been due to the high levels of endogenous H_2O_2 in SCs (Nair et al., 2019b). Further, the lack of survival-enhancing effect of NCF supernatant on NCF/SCF would be due to low levels of H_2O_2 produced/released by NCs, as reported earlier by us (Nair et al., 2019b).

In this context, it may be interesting to examine the extent of H_2O_2 diffusion during the NC-SC, SC-SC, and NC-NC interactions in liquid cultures. The presence of very low proportion of SCs and high proportion of NCs would mostly enable SC-NC and NC-NC interactions. Therefore, it is highly possible that H_2O_2 released by the SC(s) would enhance the survival of NC(s) during the SC-NC interaction but not in the NC-NC interaction. However, since mycobacteria is notorious to form clumps, the response of the bacterial cells in the clump need not iterate a similar response as in a clump-free population. Although this possibility would seem to be a limitation of the study, consistently comparable CFU values from 10 biological replicates was an indication that there were no clumps in the low density cultures used in the study. It would be interesting to study the dynamics of the SC-NC interaction in the pulmonary tuberculosis patients' sputum, where also they exist at 1:9 ratio (Vijay et al., 2014a).

4.4. The significance of katG in mediating oxidative stress survival

The conspicuous reduction in the survival of the Δ*furA-katG*/Δ*katG* NLP cells in comparison to the Δ*furA-katG*/Δ*katG* NCF cells against rifampicin and H_2O_2, revealed the role of KatG in facilitating the enhanced oxidative stress survival of the NCs. The comparable extent of survival of the Δ*furA-katG* and Δ*katG* NLP cells further strengthened the involvement of *katG* in promoting oxidative stress survival. However, a decrease in the levels of *katG* mRNA and protein was observed post 2 min exposure of the NLP cells to rifampicin and H_2O_2. We speculated that the stochastic generation of H_2O_2 as a metabolic byproduct would have caused the transient pulsing of *katG* transcription in the NCF cells. Whereas in the NLP cells, in addition to the stochastic generation of H_2O_2 as a metabolic byproduct in the NCF and SCF cells, the SCF cells would have also inherently released high levels of H_2O_2 (due to high NADH oxidase activity; Nair et al., 2019b) which might have induced the transient *katG* pulsing. However, the considerable permeability of rifampicin (Piddock et al., 2000) and H_2O_2 (Seaver and Imlay, 2001) into bacterial cells within the 2 min exposure would have probably compromised these metabolic activities of the NCF and NLP cells (Lobritz et al., 2015; Rodríguez-Rojas et al., 2020). Nevertheless, the increased levels of *katG*, which was primed by the H_2O_2 released by and present in the SCF cells' supernatant in the unstressed NLP mixture, facilitated the higher survival of the NLP cells, in comparison to the NCF cells, during the oxidative stress exposure.

In *E. coli* and other bacteria, Fur is involved in regulating iron levels in the cytoplasm (Andrews et al., 2003; McHugh et al., 2003). On the contrary, FurA in mycobacteria negatively regulates its own expression (Sala et al., 2003) and of *katG* (Zahrt et al., 2001). Thus, *furA* inactivation causes overexpression of *katG* in mycobacteria (Zahrt et al., 2001). Further, P*furA* and P*katG*, of which P*furA* is oxidative-stress-inducible, controls *katG* transcription in mycobacteria (Master et al., 2001; Milano et al., 2001). Therefore, we used the knockout mutants of both *furA-katG* and *katG* to address the role of KatG in the neutralisation of oxidative stress in the NCs. The oxidative stress tolerance was reduced in the NCs prepared from the knockout mutants where KatG function was effectively absent. This proved the role of KatG in the neutralisation of the rifampicin/H_2O_2 invoked oxidative stress in the NCs.

4.5. Stress survival facilitated by antioxidants and ROS

KatG is known to play crucial role in neutralising oxidative stress (antibiotic invoked or otherwise) in mycobacteria and other bacterial systems (Voskuil et al., 2011; Imlay, 2013; Ji et al., 2013; Khakimova et al., 2013; Dwyer et al., 2014; Martins et al., 2018). KatG overexpression conferred tolerance against ampicillin, gentamicin, and norfloxacin on the KatG mutants having significant reduction in catalytic activity and consequent low ability to suppress killing by the antibiotics (Dwyer et al., 2014). The deletion of the antioxidant enzyme superoxide dismutase (SOD) increased antibiotic lethality and abolished the emergence of genetic resisters in the stationary phase cultures of *P. aeruginosa* (Martins et al., 2018). In these lines, the present study puts forth another example of the antioxidant KatG enabling NCF cells to survive oxidative stress by neutralising the H_2O_2 generated upon rifampicin/H_2O_2 exposure.

The contribution of ROS in the antibiotic-mediated killing of bacteria is debatable (Keren et al., 2013; Liu et al., 2013). Interestingly, ROS also enhances survival against antibiotics by inducing the expression of AcrAB-TolC multidrug-resistant pump (Wu et al., 2012). ROS also decreases membrane potential and metabolism thereby increasing the density of 'persisters' in the antibiotic-exposed *E. coli* populations (Wang et al., 2017). Further, subinhibitory concentrations of superoxide generators enabled AcrAB-TolC independent pathways that enhanced the survival of antimicrobials-exposed *E. coli* cells (Mosel et al., 2013). In all these studies, it was an exogenously added oxidative stress generator that induced the antioxidants/ROS to help the bacterium survive oxidative stress. Whereas, in the present study in mycobacteria, it was the inherent, evolutionarily gained ability of SCs to produce and release significantly high levels of an ROS that enhanced the oxidative stress survival of NCs against rifampicin.

4.7. Clinical relevance of the present study

Oxidative stress tolerance exhibited by extracellular mycobacteria: The presence of mycobacteria has been documented in the extracellular milieu in animals (Lenaerts et al., 2007; Hoff et al., 2011) as well as in the environment (Velayati et al., 2015). A major proportion of the *Mtb* cells has been found to exist extracellularly in the necrotic lesions of the lung tissues in guinea pigs and mice (Lenaerts et al., 2007; Hoff et al., 2011). The priming of the NCs with enhanced oxidative stress tolerance by the SCs may possibly occur when the tubercle bacilli undergo rapid growth and division extracellularly in the host. Acquisition of antibiotic tolerance allows bacteria to thwart combination therapy (Liu et al., 2020). The presence of the SCs and the NCs in the natural 1:9 proportion in the sputum of pulmonary tuberculosis patients (Vijay et al., 2014a) cautions the possibility of occurrence of a such a tolerance-enhancing phenomenon leading to the emergence of antibiotic resisters in tuberculosis patients.

Oxidative stress tolerance exhibited by intracellular mycobacteria: The H_2O_2 produced and released by SCs would increase the survival of NCs and thereby give NCs an opportunity to survive for prolonged durations against the oxidative stress in the host. The prolonged exposure of NCs to oxidative stress might activate ROS mediated mechanisms to acquire antibiotic resister mutations as reported (Wu et al., 2012; Mosel et al., 2013; Sebastian et al., 2017; Wang et al., 2017; Nair et al., 2019b; Swaminath et al., 2020). The acquisition of antibiotic resistance by the SCs/NCs subpopulations of the saprophyte-cum-opportunistic pathogen, *M. smegmatis* (Wallace et al., 1988; Pierre-Audigier et al., 1997; Alqurashi et al., 2019), would hold good for the pathogenic *M. tuberculosis* also as the *Mtb in vitro* cultures and sputum of pulmonary tuberculosis patients contain the SCs and NCs (Vijay et al., 2014a).

Translational significance of the study: The translational significance of this study arises from the following possibilities. Firstly, the increased tolerance/survivability of the NLP cells during exposure to

exogenously added H_2O_2 indicated that the NLP cells would have an increased opportunity to survive in the host during the infection, as oxidative stress is one of the primary host defense mechanisms. The prolonged exposure of the NLP cells to oxidative stress would possibly enable the cells to enhance multiple tolerance mechanisms mediated by ROS or to acquire mutations, as reported (Wu et al., 2012; Mosel et al., 2013; Wang et al., 2017). For instance, a *katG* mutation that does not significantly compromise its catalase activity but contributes to INH resistance, as reported (Purkan et al., 2018), can emerge. Such a mutant may exhibit enhanced tolerance during INH and rifampicin exposure, which results from the induction of *katG* by the H_2O_2 secreted by the SCs in the mutant population. Multi-drug resistant isolates, which majorly harbor mutation in codon 315 of *katG* (Motavaf et al., 2021) that reduces the activation of isoniazid but maintains ~40% activity of catalase-peroxidase for its virulence (Rouse et al., 1996), support this possibility. Secondly, while many anti-tuberculosis drugs have shown differential permeability into granuloma and lung lesions, rifampicin achieved sufficient concentrations even in critical lesion compartments (Prideaux et al., 2015; Martin et al., 2016). In this context, the present work demonstrating the enhanced survival of mycobacterial cells during rifampicin exposure has potential translational significance. Thirdly, we had recently found a significantly higher resister generation frequency of NCF cells in the presence of SCF cells on exposure to rifampicin (Nair et al., 2019b), which may have arisen due to the opportunity given by *katG* gene induction to survive as tolerant cells against rifampicin exposure. It may also be noted that acquiring antibiotic tolerance allows bacteria even to override the benefits of combination therapy (Liu et al., 2020).

5. Conclusions

The present study has delineated a novel inherent mechanism of the minor subpopulation (SCs) which promotes the enhanced oxidative stress survival of the major subpopulation (NCs) in the actively growing mycobacterial cultures upon exposure to rifampicin and exogenously added H_2O_2. The SCs inherently released significantly high levels of H_2O_2 which increased the KatG levels in the NCs, thereby preparing the NCs to face the oxidative stress generated during the exposure to rifampicin and exogenously added H_2O_2.

Author contributions

PA, RRN, DS, VS, NM, KJ conceived/designed experiments; RRN, DS, VS, NM, KJ performed experiments; PA, RRN, DS, VS, NM, KJ analysed data; PA contributed reagents, materials, and analysis tools; PA, RRN, DS, VS, NM wrote the manuscript; all the authors have read and approved the manuscript.

NOTES

Authors and the funding agency do not have any competing financial interest.

CRediT authorship contribution statement

Rashmi Ravindran Nair: Conceptualization, Methodology, Data curation, Writing – original draft. **Deepti Sharan:** Methodology, Data curation, Writing – review & editing. **Vijay Srinivasan:** Methodology, Data curation. **Nagaraja Mukkayyan:** Methodology, Data curation. **Kishor Jakkala:** Methodology, Data curation. **Parthasarathi Ajitkumar:** Conceptualization, Visualization, Investigation, Supervision, Writing – review & editing.

Declaration of Competing Interest

The authors declare that they have no known competing financial interests or personal relationships that could have appeared to influence the work reported in this paper.

Acknowledgments

With highest respects and regards, PA dedicates this work as a tribute to Prof. T. Ramakrishnan (late), who led the pioneering, fundamental and foundation laying work on the biochemistry and molecular biology of *Mycobacterium tuberculosis* at Indian Institute of Science, Bangalore. **Funding:** The work was supported in part by the DBT-IISc Partnership Programme (2012-2020), research grant BT/PR23219/MED/29/1184/2017, and by the infrastructure facilities provided by the DBT-IISc Partnership Programme (2012-2020), DST-FIST, UGC-CAS, ICMR-CAS, and Indian Institute of Science, in the MCB Dep't. RRN, VS, and NM received Senior Research Fellowships from the Council of Scientific and Industrial Research (CSIR), Govt. of India. DS and KJ received Senior Research Fellowships from the University Grants Commission (UGC), Govt. of India. RRN and KJ received Research Associateship/Senior Research Fellowship from Indian Institute of Science, Bangalore and Department of Biotechnology, Government of India. PA is Emeritus Scientist of Indian Council of Medical Research (ICMR), Government of India.

Supplementary materials

Supplementary material associated with this article can be found, in the online version, at doi:10.1016/j.crmicr.2022.100148.

References

Albesa, I., Becerra, M.C., Battan, P.C., Paez, P.L., 2004. Oxidative stress involved in the antibacterial action of different antibiotics. Biochem. Biophys. Res. Commun. 317, 605–609. https://doi.org/10.1016/j.bbrc.2004.03.085.

Alqurashi, M.M., Alsaileek, A., Aljizeeri, A., Bamefleh, H.S., Alenzai, T.H., 2019. *Mycobacterium smegmatis* causing a granulomatous cardiomediastinal mass. ID Cases 18, e00608. https://doi.org/10.1016/j.idcr.2019.e00608.

Andrews, S.C., Robinson, A.K., Rodríguez-Quiñones, F., 2003. Bacterial iron homeostasis. FEMS Microbiol. Rev. 27, 215–237. https://doi.org/10.1016/S0168-6445(03)00055-X.

Ausubel, F., Kingston, R., 1989. Current protocols in molecular biology. Greene Publishing, New York, NY, p. 1987.

Höner zu Bentrup, K., Russell, D.G., 2001. Mycobacterial persistence: adaptation to a changing environment. Trends Microbiol 9, 597–605. https://doi.org/10.1016/s0966-842x(01)02238-7.

Bibb, L.A., Hatfull, G.F., 2002. Integration and excision of the *Mycobacterium tuberculosis* prophage-like element, *phiRv1*. Mol. Microbiol. 45, 1515–1526. https://doi.org/10.1046/j.1365-2958.2002.03130.x.

Blair, J.M., Webber, M.A., Baylay, A.J., Ogbolu, D.O., Piddock, L.J., 2015. Molecular mechanisms of antibiotic resistance. Nat. Rev. Microbiol. 13, 42–51. https://doi.org/10.1038/nrmicro3380.

Brauner, A., Fridman, O., Gefen, O., Balaban, N.Q., 2016. Distinguishing between resistance, tolerance and persistence to antibiotic treatment. Nat. Rev. Microbiol. 14, 320–330. https://doi.org/10.1038/nrmicro.2016.34.

Cohen, N.R., Lobritz, M.A., Collins, J.J., 2013. Microbial persistence and the road to drug resistance. Cell Host Microbe 13, 632–642. https://doi.org/10.1016/j.chom.2013.05.009.

Devi, B.G., Shaila, M.S., Ramakrishnan, T., Gopinathan, K.P., 1975. The purification and properties of peroxidase in *Mycobacterium tuberculosis* $H_{37}R_v$ and its possible role in the mechanism of action of isonicotinic acid hydrazide. Biochem. J. 149, 187–197. https://doi.org/10.1042/bj1490187.

Dwyer, D.J., Belenky, P.A., Yang, J.H., MacDonald, I.C., Martell, J.D., Takahashi, N., et al., 2014. Antibiotics induce redox-related physiological alterations as part of their lethality. Proc. Natl. Acad. Sci. U. S. A. 111, e2100–e2109. https://doi.org/10.1073/pnas.1401876111.

Ehrt, S., Schnappinger, D., Rhee, K.Y., 2018. Metabolic principles of persistence and pathogenicity in *Mycobacterium tuberculosis*. Nat. Rev. Microbiol. 16, 496–507. https://doi.org/10.1038/s41579-018-0013-4.

Erttmann, S.F., Gekera, N.O., 2019. Hydrogen peroxide release by bacteria suppresses inflammasome-dependent innate immunity. Nat. Commun. 10, 3493. https://doi.org/10.1038/s41467-019-11169-x.

Groeger, G., Quiney, C., Cotter, T.G., 2009. Hydrogen peroxide as a cell survival signaling molecule. Antioxid. Redox Signal. 11, 2655–2671.

Hoeksema, M., Brul, S., Ter Kuile, B.H., 2018. Influence of reactive oxygen species on *de novo* acquisition of resistance to bactericidal antibiotics. Antimicrob. Agents Chemother. 62, e02354–e023517. https://doi.org/10.1128/AAC.02354-17.

Hoff, D.R., Ryan, G.J., Driver, E.R., Ssemakulu, C.C., De Groote, M.A., Basaraba, R.J., et al., 2011. Location of intra- and extracellular *M. tuberculosis* populations in lungs of mice and guinea pigs during disease progression and after drug treatment. PLoS One 6, e17550. https://doi.org/10.1371/journal.pone.0017550.

Hui, J., Gordon, N., Kajioka, R., 1977. Permeability barrier to rifampin in mycobacteria. Antimicrob Agents Chemother 11, 773–779. https://doi.org/10.1128/AAC.11.5.773.

Imlay, J.A., 2013. The molecular mechanisms and physiological consequences of oxidative stress: lessons from a model bacterium. Nat. Rev. Microbiol. 11, 443–454. https://doi.org/10.1038/nrmicro3032.

Iwao, Y., Nakata, N., 2018. Roles of the three *Mycobacterium smegmatis katG* genes for peroxide detoxification and isoniazid susceptibility. Microbiol. Immunol. 62, 158–167. https://doi.org/10.1111/1348-0421.12574.

Jackson, J.H., White, C.W., Parker, N.B., Ryan, J.W., Repine, J.E., 1985. Dimethylthiourea consumption reflects H_2O_2 concentrations and severity of acute lung injury. J. Appl. Physiol. 59, 1995–1998. https://doi.org/10.1152/jappl.1985.59.6.1995.

Ji, J., Kan, S., Lee, J., Lysakowski, S., 2013. Antibiotic tolerance in *Escherichia coli* under stringent response correlates to increased catalase activity. J. Exp. Microbiol. Immunol. 17, 40–45.

Keren, I., Wu, Y., Inocencio, J., Mulcahy, L.R., Lewis, K., 2013. Killing by bactericidal antibiotics does not depend on reactive oxygen species. Science 339, 1213–1216. https://doi.org/10.1126/science.1232688.

Khakimova, M., Ahlgren, H.G., Harrison, J.J., English, A.M., Nguyen, D., 2013. The stringent response controls catalases in *Pseudomonas aeruginosa* and is required for hydrogen peroxide and antibiotic tolerance. J. Bacteriol. 195, 2011–2020. https://doi.org/10.1128/JB.02061-12.

Kohanski, M.A., DePristo, M.A., Collins, J.J., 2010. Sublethal antibiotic treatment leads to multidrug resistance via radical-induced mutagenesis. Mol. Cell 37, 311–320.

Lenaerts, A.J., Hoff, D., Aly, S., Ehlers, S., Andries, K., Cantarero, L., et al., 2007. Location of persisting mycobacteria in a guinea pig model of tuberculosis revealed by R207910. Antimicrob. Agents Chemother. 51, 3338–3345. https://doi.org/10.1128/AAC.00276-07.

Li, X., Wu, J., Han, J., Hu, Y., Mi, K., 2015. Distinct responses of *Mycobacterium smegmatis* to exposure to low and high levels of hydrogen peroxide. PLoS One 10, e0134595. https://doi.org/10.1371/journal.pone.0134595.

Liu, J., Gefen, O., Ronin, I., Bar-Meir, M., Balaban, N.Q., 2020. Effect of tolerance on the evolution of antibiotic resistance under drug combinations. Science 367, 200–204. https://doi.org/10.1126/science.aay3041.

Liu, Y., Imlay, J.A., 2013. Cell death from antibiotics without the involvement of reactive oxygen species. Science 339, 1210–1213. https://doi.org/10.1126/science.1232751.

Lobritz, M.A., Belenky, P., Porter, C.B., Gutierrez, A., Yang, J.H., Schwarz, E.G., et al., 2015. Antibiotic efficacy is linked to bacterial cellular respiration. Proc. Natl. Acad. Sci. U. S. A. 112, 8173–8180. https://doi.org/10.1073/pnas.1509743112.

Manca, C., Paul, S., Barry, 3rd., Freedman, V.H., Kaplan, G., 1999. *Mycobacterium tuberculosis* catalase and peroxidase activities and resistance to oxidative killing in human monocytes *in vitro*. Infect. Immun. 67, 74–79. https://doi.org/10.1128/IAI.67.1.74-79.1999.

Marinho, H.S., Real, C., Cyrne, L., Soares, H., Antunes, F., 2014. Hydrogen peroxide sensing, signaling, and regulation of transcription factors. Redox Biol 2, 535–562. https://doi.org/10.1016/j.redox.2014.02.006.

Martin, C.J., Carey, A.F., Fortune, S.M., 2016. A bug's life in the granuloma. Seminars in Immunopath 38, 213–220. https://doi.org/10.1007/s00281-015-0533-1.

Martins, D., McKay, G., Sampathkumar, G., Khakimova, M., English, A.M., Nguyen, D., 2018. Superoxide dismutase activity confers (p)ppGpp-mediated antibiotic tolerance to stationary-phase *Pseudomonas aeruginosa*. Proc. Natl. Acad. Sci. U. S. A. 115, 9797–9802. https://doi.org/10.1073/pnas.1804525115.

Master, S., Zahrt, T.C., Song, J., Deretic, V., 2001. Mapping of *Mycobacterium tuberculosis katG* promoters and their differential expression in infected macrophages. J. Bacteriol. 183, 4033–4039. https://doi.org/10.1128/JB.183.13.4033-4039.2001.

McBee, M.E., Chionh, Y.H., Sharaf, M.L., Ho, P., Cai, M.W.L., Dedon, P.C., 2017. Production of superoxide in bacteria is stress- and cell state-dependent: a gating-optimised flow cytometry method that minimises ROS measurement artifacts with fluorescent dyes. Front Microbiol 8, 459.

McHugh, J.P., Rodríguez-Quiñones, F., Abdul-Tehrani, H., Svistunenko, D.A., Poole, R. K., Cooper, C.E., et al., 2003. Global iron-dependent gene regulation in *Escherichia coli*: A new mechanism for iron homeostasis. J. Biol. Chem. 278, 29478–29486. https://doi.org/10.1074/jbc.M303381200.

Milano, A., Forti, F., Sala, C., Riccardi, G., Ghisotti, D., 2001. Transcriptional regulation of *furA* and *katG* upon oxidative stress in *Mycobacterium smegmatis*. J. Bacteriol. 183, 6801–6806. https://doi.org/10.1128/JB.183.23.6801-6806.2001.

Mosel, M., Li, L., Drlica, K., Zhao, X., 2013. Superoxide-mediated protection of *Escherichia coli* from antimicrobials. Antimicrob. Agents Chemother. 57, 5755–5759. https://doi.org/10.1128/AAC.00754-13.

Motavaf, B., Keshavarz, N., Ghorbanian, F., Firuzabadi, S., Hosseini, F., Bostanabad, S.Z., 2021. Detection of genomic mutations in *katG* and *rpoB* genes among multidrug-resistant *Mycobacterium tuberculosis* isolates from Tehran, Iran. New Microbes New Infect. 41, 100879 https://doi.org/10.1016/j.nmni.2021.100879.

Nair, R.R., Sharan, D., Ajitkumar, P., 2019b. A minor subpopulation of mycobacteria inherently produces high levels of reactive oxygen species that generate antibiotic resisters at high frequency from itself and enhance resister generation from its major kin subpopulation. Front. Microbiol. 10, 1842. https://doi.org/10.3389/fmicb.2019.01842.

Nair, R.R., Sharan, D., Sebastian, J., Swaminath, S., Ajitkumar, P., 2019a. Heterogeneity of ROS levels in antibiotic-exposed mycobacterial subpopulations confers differential susceptibility. Microbiology 165, 668–682. https://doi.org/10.1099/mic.0.000797.

Nakagawa, H., Hasumi, K., Woo, J.-T., Nagai, K., Wachi, M., 2004. Generation of hydrogen peroxide primarily contributes to the induction of Fe (II)-dependent apoptosis in Jurkat cells by (-) epigallocatechin gallate. Carcinogenesis 25, 1567–1574. https://doi.org/10.1093/carcin/bgh168.

Nicoloff, H., Hjort, K., Levin, B.R., Andersson, D.I., 2019. The high prevalence of antibiotic heteroresistance in pathogenic bacteria is mainly caused by gene amplification. Nat. Microbiol. 4, 504–514. https://doi.org/10.1038/s41564-018-0342-0.

Parker, N.B., Berger, E.M., Curtis, W.E., Muldrow, M.E., Linas, S.L., Repine, J.E., 1985. Hydrogen peroxide causes dimethylthiourea consumption while hydroxyl radical causes dimethyl sulfoxide consumption *in vitro*. J. Free Radic. Biol. Med. 1, 415–419. https://doi.org/10.1016/0748-5514(85)90155-2.

Paul, A., Nair, R.R., Ajitkumar, P., 2021. Genetic resisters to antibiotics in *Escherichia coli* arise from the antibiotic-surviving population containing three reactive oxygen species. FEMS Microbiol. Lett. 368, fnab157. https://doi.org/10.1093/femsle/fnab157.

Paul, A., Nair, R.R., Jakkala, K., Pradhan, A., Ajitkumar, P., 2022. Elevated levels of three reactive oxygen species and Fe (II) in the antibiotic-surviving population of mycobacteria facilitate de novo emergence of genetic resisters to antibiotics. Antimicrob. Agents Chemother. doi: 10.1128/aac.02285-21.

Piccaro, G., Pietraforte, D., Giannoni, F., Mustazzolu, A., Fattorini, L., 2014. Rifampin induces hydroxyl radical formation in *Mycobacterium tuberculosis*. Antimicrob. Agents Chemother. 58, 7527–7533. https://doi.org/10.1128/AAC.03169-14.

Piddock, L.J., Williams, K.J., Ricci, V., 2000. Accumulation of rifampicin by *Mycobacterium aurum, Mycobacterium smegmatis* and *Mycobacterium tuberculosis*. J. Antimicrob. Chemother. 45, 159–165. https://doi.org/10.1093/jac/45.2.159.

Pierre-Audigier, C., Jouanguy, E., Lamhamedi, S., Altare, F., Rauzier, J., Vincent, V., et al., 1997. Fatal disseminated *Mycobacterium smegmatis* infection in a child with inherited interferon gamma receptor deficiency. Clin. Infect.Dis. 24, 982–984.

Pillai-Kastoori, L., Schutz-Geschwender, A.R., Harford, J.A., 2020. A systematic approach to quantitative Western blot analysis. Anal. Biochem. 593, 113608 https://doi.org/10.1016/j.ab.2020.113608.

Prideaux, B., Via, L.E., Zimmerman, M.D., Eum, S., Sarathy, J., O'Brien, P., et al., 2015. The association between sterilizing activity and drug distribution into tuberculosis lesions. Nature Med 21, 1223–1227. https://doi.org/10.1038/nm.3937.

Purkan, P., Ihsanawati, I., Natalia, D., Syah, Y.M., Retnoningrum, D.S., Siswanto, I., 2018. Molecular Analysis of *katG* Encoding Catalase-Peroxidase from Clinical Isolate of Isoniazid-Resistant *Mycobacterium tuberculosis*. J. Med. Life 11, 160–167.

Rodríguez-Rojas, A., Kim, J.J., Johnston, P.R., Makarova, O., Eravci, M., Weise, C., et al., 2020. Non-lethal exposure to H2O2 boosts bacterial survival and evolvability against oxidative stress. PLoS Genet 16, e1008649. https://doi.org/10.1371/journal.pgen.1008649.

Rouse, D.A., DeVito, J.A., Li, Z., Byer, H., Morris, S.L., 1996. Site-directed mutagenesis of the *katG* gene of *Mycobacterium tuberculosis*: effects on catalase-peroxidase activities and isoniazid resistance. Mol. Microbiol. 22, 583–592. https://doi.org/10.1046/j.1365-2958.1996.00133.x.

Roy, S., Narayana, Y., Balaji, K.N., Ajitkumar, P., 2012. Highly fluorescent GFP_m^{2+} -based genome integration-proficient promoter probe vector to study *Mycobacterium tuberculosis* promoters in infected macrophages. Microbial Biotechnol 5, 98–105. https://doi.org/10.1111/j.1751-7915.2011.00305.x.

Sala, C., Forti, F., Di Florio, E., Canneva, F., Milano, A., Riccardi, G., 2003. *Mycobacterium tuberculosis furA* autoregulates its own expression. J. Bacteriol. 185, 5357–5362. https://doi.org/10.1128/JB.185.18.5357-5362.2003.

Sambrook, J., Russell, D.W., 2001. Molecular Cloning: A Laboratory Manual, 3rd ed. Cold Spring Harbor Laboratory Press.

Sarathy, J.P., Dartois, V., Lee, E.J., 2012. The role of transport mechanisms in *Mycobacterium tuberculosis* drug resistance and tolerance. Pharmaceuticals 5, 1210–1235. https://doi.org/10.3390/ph5111210.

Seaver, L.C., Imlay, J.A., 2001. Hydrogen peroxide fluxes and compartmentalization inside growing *Escherichia coli*. J. Bacteriol. 183, 7182–7189. https://doi.org/10.1128/JB.183.24.7182-7189.2001.

Sebastian, J., 2016. Response of *Mycobacterium tuberculosis* to rifampicin - a cellular, molecular, and ultrastructural study. PhD Thesis submitted to Indian Institute of Science, Bangalore, India.

Sebastian, J., Swaminath, S., Nair, R.R., Jakkala, K., Pradhan, A., Ajitkumar, P., 2017. *De novo* emergence of genetically resistant mutants of *Mycobacterium tuberculosis* from the persistence phase cells formed against antituberculosis drugs in vitro. Antimicrob. Agents Chemother. 61, e01343–e013416. https://doi.org/10.1128/AAC.01343-16.

Sebastian, J., Nair, R.R., Swaminath, S., Ajitkumar, P., 2020. *Mycobacterium tuberculosis* cells surviving in the continued presence of bactericidal concentrations of rifampicin in vitro develop negatively charged thickened capsular outer layer that restricts permeability to the antibiotic. Front. Microbiol. 11, 554795 https://doi.org/10.3389/fmicb.2020.554795.

Sies, H., 2017. Hydrogen peroxide as a central redox signaling molecule in physiological oxidative stress: oxidative eustress. Redox Biol 11, 613–619. https://doi.org/10.1016/j.redox.2016.12.035.

Şimşek, E., Kim, M., 2018. The emergence of metabolic heterogeneity and diverse growth responses in isogenic bacterial cells. ISME J 12, 1199–1209. https://doi.org/10.1038/s41396-017-0036-2.

Snapper, S.B., Melton, R.E., Mustafa, S., Kieser, T., Jacobs, W.R.J., 1990. Isolation and characterization of efficient plasmid transformation mutants of *Mycobacterium smegmatis*. Mol. Microbiol. 4, 1911–1919. https://doi.org/10.1111/j.1365-2958.1990.tb02040.x.

Swaminath, S., Paul, A., Pradhan, A., Sebastian, J., Nair, R.R., Ajitkumar, P., 2020. *Mycobacterium smegmatis* moxifloxacin persister cells produce high levels of hydroxyl radical, generating genetic resisters selectable not only with moxifloxacin, but also

with ethambutol and isoniazid. Microbiology 166, 180–198. https://doi.org/10.1099/mic.0.000874.
Sylte, M.J., Inzana, T.J., Czuprynski, C.J., 2004. Reactive oxygen and nitrogen intermediates contribute to *Haemophilus somnus* lipooligosaccharide-mediated apoptosis of bovine endothelial cells. Vet. Immunol. Immunopathol. 97, 207–217. https://doi.org/10.1016/j.vetimm.2003.09.005.
van Kessel, J.C., Hatfull, G.F., 2007. Recombineering in *Mycobacterium tuberculosis*. Nat. Methods 4, 147–152. https://doi.org/10.1038/nmeth996.
Velayati, A.A., Farnia, P., Mirsaeidi, M., 2015. Persistence of *Mycobacterium tuberculosis* in environmental samples. Int. J. Mycobacteriol. 4, 1. https://doi.org/10.1016/j.ijmyco.2014.11.005.
Vijay, S., Mukkayyan, N., Ajitkumar, P., 2014b. Highly deviated asymmetric division in very low proportion of mycobacterial mid-log phase cells. Open Microbiol. J. 8, 40–50. https://doi.org/10.2174/1874285801408010040.
Vijay, S., Nagaraja, M., Sebastian, J., Ajitkumar, P., 2014a. Asymmetric cell division in Mycobacterium tuberculosis and its unique features. Arch. Microbiol. 196, 157–168. https://doi.org/10.1007/s00203-014-0953-7.
Vijay, S., Nair, R.R., Sharan, D., Jakkala, K., Mukkayyan, N., Swaminath, S., et al., 2017. Mycobacterial cultures contain cell size and density specific sub-populations of cells with significant differential susceptibility to antibiotics, oxidative and nitrite stress. Front. Microbiol. 8, 463. https://doi.org/10.3389/fmicb.2017.00463.
Voelz, K., Johnston, S.A., Smith, L.M., Hall, R.A., Idnurm, A., May, R.C., 2014. Division of labour" in response to host oxidative burst drives a fatal *Cryptococcus gattii* outbreak. Nat. Commun. 5, 5194. https://doi.org/10.1038/ncomms6194.
Voskuil, M.I., Bartek, I.L., Visconti, K., Schoolnik, G.K., 2011. The response of *Mycobacterium tuberculosis* to reactive oxygen and nitrogen species. Front. Microbiol. 2, 105. https://doi.org/10.3389/fmicb.2011.00105.
Wakamoto, Y., Dhar, N., Chait, R., Schneider, K., Signorino-Gelo, F., Leibler, S., et al., 2013. Dynamic persistence of antibiotic-stressed mycobacteria. Science 339, 91–95. https://doi.org/10.1126/science.1229858.
Wallace, R.J., Nash, D.R., Tsukamura, M., Blacklock, Z.M., Silcox, V.A., 1988. Human disease due to *Mycobacterium smegmatis*. J. Infect. Dis. 158, 52–59. https://doi.org/10.1093/infdis/158.1.52.
Wang, T., El Meouche, I., Dunlop, M.J., 2017. Bacterial persistence induced by salicylate via reactive oxygen species. Sci. Rep. 7, 43839. https://doi.org/10.1038/srep43839.
Wang, W., Chen, K., Xu, C., 2006. DNA quantification using EvaGreen and a real-time PCR instrument. Anal. Biochem. 356, 303–305. https://doi.org/10.1016/j.ab.2006.05.027.
Weart, R.B., Levin, P.A., 2003. Growth rate-dependent regulation of medial FtsZ ring formation. J. Bacteriol. 185, 2826–2834. https://doi.org/10.1128/JB.185.9.2826-2834.2003.
Wecker, E., 1959. The extraction of infectious virus nucleic acid with hot phenol. Virology 7, 241–243. https://doi.org/10.1016/0042-6822(59)90191-6.
Willems, E., Leyns, L., Vandesompele, J., 2008. Standardization of real-time PCR gene expression data from independent biological replicates. Anal. Biochem. 379, 127–129. https://doi.org/10.1016/j.ab.2008.04.036.
Woodford, N., Ellington, M.J., 2007. The emergence of antibiotic resistance by mutation. Clin. Microbiol. Infect. 13, 5–18. https://doi.org/10.1111/j.1469-0691.2006.01492.x.
Wu, Y., Vulić, M., Keren, I., Lewis, K., 2012. Role of oxidative stress in persister tolerance. Antimicrob. Agents Chemother. 56, 4922–4926. https://doi.org/10.1128/AAC.00921-12.
Zahrt, T.C., Song, J., Siple, J., Deretic, V., 2001. Mycobacterial FurA is a negative regulator of catalase-peroxidase gene katG. Mol. Microbiol. 39, 1174–1185. https://doi.org/10.1111/j.1365-2958.2001.02321.x.
Zhang, Y., Heym, B., Allen, B., Young, D., Cole, S., 1992. The catalase-peroxidase gene and isoniazid resistance of *Mycobacterium tuberculosis*. Nature 358, 591–593. https://doi.org/10.1038/358591a0.
Zhao, X., Yu, H., Yu, S., Wang, F., Sacchettini, J.C., Magliozzo, R.S., 2006. Hydrogen peroxide-mediated isoniazid activation catalyzed by *Mycobacterium tuberculosis* catalase-peroxidase (KatG) and its S315T mutant. Biochemistry 45, 4131–4140. https://doi.org/10.1021/bi051967o.